

AD-755 746

FERROELECTRIC DISPLAYS

Maurice H. Francombe, et al

Westinghouse Research Laboratories

Prepared for:

Office of Naval Research

December 1972

DISTRIBUTED BY:

**NTIS**

National Technical Information Service  
U. S. DEPARTMENT OF COMMERCE  
5285 Port Royal Road, Springfield Va. 22151

AD 755746

FERROELECTRIC DISPLAYS

Final Report

Research Sponsored by the  
Office of Naval Research

Contract N00014-71-C-0268  
Contract Authority NR215-180

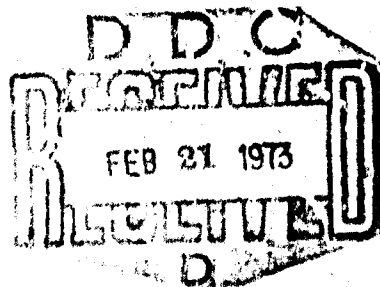
Period Covered: 15 April 1971 through 14 April 1972

M. H. Francombe, S. Y. Wu and W. J. Takei  
Westinghouse Research Laboratories

December 1972

Reproduced by  
NATIONAL TECHNICAL  
INFORMATION SERVICE  
U S Department of Commerce  
Springfield VA 22151

Approved for public release; distribution unlimited



Subj: Annual Technical Report, Contract N00014-71-C-0268,  
NR 215-180; approval for distribution

N O T I C E

Change of Address

Organizations receiving reports on initial distribution list should confirm correct address. This list is located at the end of the report. Any change of address or distribution should be conveyed to the Office of Naval Research, Code 461, Arlington, Virginia 22217.

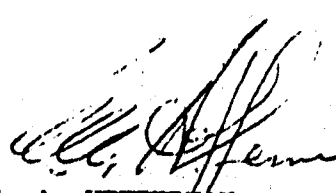
Disposition

When this report is no longer needed, it may be transmitted to other organizations. Do not return it to the originator or the monitoring office.

Disclaimer

The findings in this report are not to be construed as an official Department of Defense or Navy Department position unless as designated by other official documents.

APPROPRIATION for	
NTIS-	White Section <input checked="" type="checkbox"/>
OC	Buff Section <input type="checkbox"/>
SECURITY	<input type="checkbox"/>
.....	
BY	
.....	
REVIEW/AVAILABILITY CODES	
.....	
SPECIAL	
.....	

  
G. A. HEFFERNAN  
By direction

UNCLASSIFIED

Security Classification

DOCUMENT CONTROL DATA - R&D		
(Security classification of title, body of abstract and indexing annotation must be entered when the overall report is classified)		
1 ORIGINATING ACTIVITY (Corporate author) Westinghouse Electric Corporation Research and Development Center Pittsburgh, Pennsylvania 15235		2a REPORT SECURITY CLASSIFICATION Unclassified
		2b GROUP
3 REPORT TITLE  FERROELECTRIC DISPLAYS		
4 DESCRIPTIVE NOTES (Type of report and inclusive dates) Final Report (15 April 1971 to 14 April 1972)		
5 AUTHOR(S) (Last name, first name, initial) Francombe, Maurice H. Wu, Shu Y. Takei, William J.		
6 REPORT DATE December 1972	7a TOTAL NO OF PAGES 78	7b NO OF REFS 33
8a CONTRACT OR GRANT NO. N00014-71-C-0268	9a ORIGINATOR'S REPORT NUMBER(S)	
b PROJECT NO NR 215-180		
c	9b OTHER REPORT NO(S) (Any other numbers that may be assigned this report)	
d		
10 AVAILABILITY/LIMITATION NOTICES  Approved for public release; distribution unlimited		
11. SUPPLEMENTARY NOTES Details of illustrations in this document may be better studied on microfiche	12. SPONSORING MILITARY ACTIVITY Office of Naval Research Arlington, Virginia 22217	
13 ABSTRACT  Two ferroelectric materials, single-crystal bismuth titanate and hot-pressed ceramic lead-zirconate-titanate of approximately 65:35 composition modified with lanthanum oxide (PLZT), have potential applications in non-volatile optical display and memory devices. The goal of the present program is to develop optical projection display structures (5 x 7 in.) which can function in solid-state real-time aircraft instrumentation systems. Display structures have been fabricated using both optical and matrix addressing techniques requiring optimization of the preparation and delineation of various components such as transparent or opaque conductors, photoconductors, and opaque insulators.  Evaluation of commercially available hot pressed PLZT ceramics showed them to possess poor electro-optic switching properties. That this is not due to difficulties in the device structure has been shown by simplified configurations using direct application of electric fields. These results are attributed to poor control of grain size uniformity and the most recently obtained sample shows improved though not optimum properties.  Techniques have been perfected in these laboratories under an Air Force contract to prepare epitaxial bismuth titanate films. By growth on spinel substrates under special conditions, it has been possible to achieve single domain (010) films required for the unique extinction display mode with properties comparable to those obtained in bulk crystals. Fabrication of an interdigitated electrode structure has demonstrated good ON/OFF characteristics as well as a grey scale capability.		

DD FORM 1 JAN 64 1473

I

UNCLASSIFIED

Security Classification

RM 35054

14 KEY WORDS	LINK A		LINK B		LINK C	
	ROLE	WT	ROLE	WT	ROLE	WT
displays						
ferroelectrics						
lead zirconate titanate						
bismuth titanate						
electro-optic switching						
matrix address						
optical address						
display fabrication						

### INSTRUCTIONS

1. **ORIGINATING ACTIVITY:** Enter the name and address of the contractor, subcontractor, grantee, Department of Defense activity or other organization (*corporate author*) issuing the report.
- 2a. **REPORT SECURITY CLASSIFICATION:** Enter the overall security classification of the report. Indicate whether "Restricted Data" is included. Marking is to be in accordance with appropriate security regulations.
- 2b. **GROUP:** Automatic downgrading is specified in DoD Directive 5200.10 and Armed Forces Industrial Manual. Enter the group number. Also, when applicable, show that optional markings have been used for Group 3 and Group 4 as authorized.
3. **REPORT TITLE:** Enter the complete report title in all capital letters. Titles in all cases should be unclassified. If a meaningful title cannot be selected without classification, show title classification in all capitals in parenthesis immediately following the title.
4. **DESCRIPTIVE NOTES:** If appropriate, enter the type of report, e.g., interim, progress, summary, annual, or final. Give the inclusive dates when a specific reporting period is covered.
5. **AUTHOR(S):** Enter the name(s) of author(s) as shown on or in the report. Enter last name, first name, middle initial. If military, show rank and branch of service. The name of the principal author is an absolute minimum requirement.
6. **REPORT DATE:** Enter the date of the report as day, month, year; or month, year. If more than one date appears on the report, use date of publication.
- 7a. **TOTAL NUMBER OF PAGES:** The total page count should follow normal pagination procedures, i.e., enter the number of pages containing information.
- 7b. **NUMBER OF REFERENCES:** Enter the total number of references cited in the report.
- 8a. **CONTRACT OR GRANT NUMBER:** If appropriate, enter the applicable number of the contract or grant under which the report was written.
- 8b, 8c, & 8d. **PROJECT NUMBER:** Enter the appropriate military department identification, such as project number, subproject number, system numbers, task number, etc.
- 9a. **ORIGINATOR'S REPORT NUMBER(S):** Enter the official report number by which the document will be identified and controlled by the originating activity. This number must be unique to this report.
- 9b. **OTHER REPORT NUMBER(S):** If the report has been assigned any other report numbers (*either by the originator or by the sponsor*), also enter this number(s).
10. **AVAILABILITY/LIMITATION NOTICES:** Enter any limitations on further dissemination of the report, other than those

imposed by security classification, using standard statements such as:

- (1) "Qualified requesters may obtain copies of this report from DDC."
- (2) "Foreign announcement and dissemination of this report by DDC is not authorized."
- (3) "U. S. Government agencies may obtain copies of this report directly from DDC. Other qualified DDC users shall request through \_\_\_\_\_."
- (4) "U. S. military agencies may obtain copies of this report directly from DDC. Other qualified users shall request through \_\_\_\_\_."
- (5) "All distribution of this report is controlled. Qualified DDC users shall request through \_\_\_\_\_."

If the report has been furnished to the Office of Technical Services, Department of Commerce, for sale to the public, indicate this fact and enter the price, if known.

11. **SUPPLEMENTARY NOTES:** Use for additional explanatory notes.

12. **SPONSORING MILITARY ACTIVITY:** Enter the name of the departmental project office or laboratory sponsoring (*paying for*) the research and development. Include address.

13. **ABSTRACT:** Enter an abstract giving a brief and factual summary of the document indicative of the report, even though it may also appear elsewhere in the body of the technical report. If additional space is required, a continuation sheet shall be attached.

It is highly desirable that the abstract of classified reports be unclassified. Each paragraph of the abstract shall end with an indicator of the military security classification of the information in the paragraph, represented as (TS), (S), (C), or (U).

There is no limitation on the length of the abstract. However, the suggested length is from 150 to 225 words.

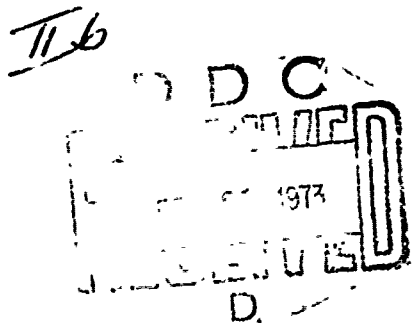
14. **KEY WORDS:** Key words are technically meaningful terms or short phrases that characterize a report and may be used as index entries for cataloging the report. Key words must be selected so that no security classification is required. Identifiers, such as equipment model designation, trade name, military project code name, geographic location, may be used as key words but will be followed by an indication of technical content. The assignment of links, rules, and weights is optional.

*na*

FERROELECTRIC DISPLAYS

M. H. Francombe, S. Y. Wu and W. J. Takei

Approved for public release; distribution unlimited.



## FOREWORD

This report was prepared by the Westinghouse Research Laboratories, Pittsburgh, Pennsylvania, 15235, under United States Department of the Navy Contract N00014-71-C-0268 Ferroelectric Displays. The work was administered under the direction of the Office of Naval Research, Arlington, Virginia, 22217. The Technical Program Monitor was initially Lt. CDR. H. B. Lyon and subsequently Lt. CDR. R. E. Hudson with Contract Authority No. NR 215-180.

This report covers work performed between 15 April 1971 and 14 April 1972 and was submitted by the authors in June 1972.

Significant contributions were made by P. D. Blais, A. J. Noreika, C. M. Pedersen, G. Ferguson, J. H. Rieger, J. C. Neidigh, and W. P. Duckstein.

### SUMMARY

Two ferroelectric materials, single-crystal bismuth titanate and hot-pressed ceramic lead-zirconate-titanate of approximately 65:35 composition modified with lanthanum oxide (PLZT), have potential applications in non-volatile optical display and memory devices. The goal of the present program is to develop optical projection display structures (5 x 7 in.) which can function in solid-state real-time aircraft instrumentation systems. Display structures have been fabricated using both optical and matrix addressing techniques requiring optimization of the preparation and delineation of various components such as transparent or opaque conductors, photoconductors, and opaque insulators.

Evaluation of commercially available hot pressed PLZT ceramics showed them to possess poor electro-optic switching properties. That this is not due to difficulties in the device structure has been shown by simplified configurations using direct application of electric fields. These results are attributed to poor control of grain size uniformity and the most recently obtained sample shows improved though not optimum properties.

Techniques have been perfected in these laboratories under an Air Force contract to prepare epitaxial bismuth titanate films. By growth on spinel substrates under special conditions, it has been possible to achieve single domain (010) films required for the unique extinction display mode with properties comparable to those obtained in bulk crystals. Fabrication of an interdigitated electrode structure has demonstrated good ON/OFF characteristics as well as a gray scale capability.

## TABLE OF CONTENTS

	<u>Page</u>
I. INTRODUCTION -- GENERAL STATUS OF DISPLAYS . . . . .	1
II. STATUS OF FERROELECTRIC DISPLAYS . . . . .	5
II.1 INTRODUCTION . . . . .	5
II.2 SINGLE CRYSTAL FERROELECTRICS . . . . .	8
II.3 POLYCRYSTALLINE FERROELECTRICS . . . . .	14
III. AIMS OF PRESENT STUDY . . . . .	19
III.1 OPTIMIZATION OF FERROELECTRIC MATERIAL . . . . .	20
III.2 DESIGN AND PREPARATION OF EXPERIMENTAL DISPLAY DEVICES . . . . .	21
III.3 DISPLAY CHARACTERISTICS WITH OPTICAL ADDRESS . . . . .	21
III.4 MATRIX ELECTRODE ADDRESS . . . . .	22
IV. MATERIALS STUDIES . . . . .	23
IV.1 INTRODUCTION -- MATERIAL PARAMETER REQUIREMENTS . . . . .	23
IV.2 PLZT FERROELECTRIC CERAMICS . . . . .	27
IV.3 EPITAXIAL BISMUTH TITANATE FILMS . . . . .	33
IV.4 PHOTOCONDUCTORS . . . . .	36
a) ZnSe . . . . .	36
b) PVK . . . . .	40
c) CdS . . . . .	41
IV.5 TRANSPARENT CONDUCTIVE FILMS . . . . .	43
IV.6 OPAQUE GaAs AND INSULATING SiO <sub>2</sub> MULTILAYERS . . . . .	47
V. EVALUATION OF DISPLAY PROPERTIES . . . . .	53
V.1 TEST RESULTS ON PLZT FINE-GRAINED CERAMICS . . . . .	53
a) OPTICAL ADDRESS STUDIES . . . . .	53

**Preceding page blank**

	<u>Page</u>
b) ADDRESS VIA IDT AND MATRIX ELECTRODE STRUCTURES . .	57
c) TESTS ON PLZT COARSE-GRAINED CERAMICS . . . . .	62
V.2 TEST RESULTS ON EPITAXIAL BISMUTH TITANATE FILMS . . .	65
V.3 EXPERIMENTAL DISPLAY STRUCTURES . . . . .	69
VI. CONCLUSIONS AND RECOMMENDATIONS FOR FURTHER WORK . . . . .	75
REFERENCES . . . . .	76

# LIST OF FIGURES

	<u>Page</u>
Fig. 1 A $\text{Bi}_4\text{Ti}_3\text{O}_{12}$ crystal viewed along the "b" axis. The X-Y axes show the different optical indicatrix positions for opposite saturation states on the hysteresis loop. Viewing in crossed polarized light with the polarizers aligned on one of the extinction positions provides a direct nondestructive readout of the ferroelectric polarization state [after Cummins, Ref. (12)].	10
Fig. 2 Arrangement for producing domain contrast by differential-retardation in bismuth titanate crystal. View of crystal is along <u>b</u> -axis, light is incident in the a-c plane (after Cummins and Luke, Ref. 17).	12
Fig. 3 Portion of configuration used by Meitzler et al. <sup>(27)</sup> for PZT optical display device.	17
Fig. 4 Schematic diagram of the PC-FE device structure.	24
Fig. 5 Etched microstructures of fine-grained PLZT ceramics. (a) Vernitron material and (b) Honeywell material.	29
Fig. 6 Etched microstructures of coarse-grained PLZT ceramics. (a) early Honeywell material, (b) latest Honeywell material, and (c) Sandia material. <sup>(30)</sup>	30
Fig. 7 Hysteresis loop observed on latest Honeywell coarse-grained ceramics. Scale: vertical, $20 \mu\text{C}/\text{cm}^2$ and horizontal, 2.35 KV/cm.	32
Fig. 8 Dielectric constant and dissipation factor versus frequency of a 8/65/35 PLZT (Vernitron).	34
Fig. 9 Microstructure under crossed polarizers of bismuth titanate films grown on (110) MgO. Elongated regions are <u>a</u> -up regions and the background is <u>4</u> -up regions.	35
Fig. 10 Scheme of vacuum evaporation within a hot chamber for ZnSe films.	38
Fig. 11 Typical 40 HZ hysteresis loops of ferroelectric (PLZT) - photoconductor (ZnSe) sandwiched device. Inner loop is in the dark and outer loop is under light illumination.	40
Fig. 12 Room temperature resistivity of indium-oxide films versus the substrate deposition temperature.	46

	<u>Page</u>
Fig. 13 Delineated tin-oxide doped indium oxide pattern after being etched with oxalic acid. The width of the strip line is 12 $\mu\text{m}$ .	47
Fig. 14 Photographs of tin oxide doped indium oxide films deposited on photoresist pattern.	49
Fig. 15 Tin oxide doped indium oxide pattern delineated with rejection technique. The width of the strip line is 10 $\mu\text{m}$ .	50
Fig. 16 Photograph of PLZT windows. The dead areas are blocked with GaAs-SiO <sub>2</sub> multilayer.	54
Fig. 17 Interdigital finger array used for bottom switching electrodes.	55
Fig. 18 A PLZT sample with top and bottom crossed interdigital finger array electrodes.	59
Fig. 19 A PLZT sample with 10 mils by 10 mils windows.	61
Fig. 20 Contrast ratio versus switching electric field measured on a 100 $\mu\text{m}$ coarse-grained sample.	64
Fig. 21 Maximum contrast ratio versus the sample thickness. [Solid lines after Smith and Land (20)].	66
Fig. 22 The test structure used to observe the contrast effect of epitaxial (010) bismuth titanate films.	68
Fig. 23 Typical contrast ratio versus switching field on a bismuth titanate film with interdigital electrode structure.	70
Fig. 24 Electrode geometry designed for use with (010) bismuth titanate films with X-Y matrix address.	72
Fig. 25 Photograph of a bismuth titanate sample after the top electrodes are delineated.	73

## I. INTRODUCTION -- GENERAL STATUS OF DISPLAYS

During recent years the requirements of both military and commercial systems have accelerated the interest in solid state optical display and memory storage concepts. A wide range of phenomena has been considered, such as magneto-optic, electro-optic, photochromic, photoconductive, electromechanical (reflective), and luminescent. In several cases, extensive effort has been invested in optimizing material preparation, in characterizing optical properties, and in developing storage, address and erase procedures suitable for specific device applications. Typical examples of such efforts are the current widespread research and development activities in bubble domain memories and in ferroelectric optical display and memory systems.

In the case of real-time optical display systems, initial consideration is invariably given to the cathode ray tube (CRT) as a means of addressing the display medium. This is not necessarily because of the fundamental advantages of CRT approach but also because of the practical consideration that it has been developed to a degree unmatched by any other technique. The primary impetus for continuing development in CRT technology is the large demand created by the home TV market. While CRT systems have attained great sophistication, and improvements are still being made, the more demanding requirements of modern display applications have begun to emphasize fundamental difficulties. Among these might be mentioned the lack of inherent storage capability, the need for a vacuum system, and a severe limitation in light levels, which in turn limits projection possibilities.

An effective summary of the present situation with respect to display systems has been given by a special issue on the IEEE Transactions on Electron Devices, ED 18, September 1971.

The various types of display systems currently under investigation can conveniently be classified under two categories; either they generate their own light and give the desired image directly, as does a CRT, or they act like a movie system (or slide projector for slower techniques) with the optically active material acting as a light modulating film frame whose image can be continuously changed. The greatest development has probably been made in the first class of displays. Many different electroluminescent materials have been investigated for this application, basically II-VI or III-V compounds which emit light when subjected to appropriate electric fields. Plasma display panels generate light via a controlled, localized glow discharge in a gas. While in principle, both types of displays could present pictorial information, practical application thus far has been limited to alphanumeric and simple symbolic outputs.

Most of the new display techniques under investigation permit localized control of the transmission of viewing light beam which is then projected for display magnification or viewed directly. Ferroelectrics for this purpose are discussed in the next section. Liquid crystals are fundamentally different but phenomenologically similar in that, like some ferroelectrics, they exhibit controllable birefringence and light scattering changes which can be utilized. Color centers introduced by light beams (photochromism) and electron beams

(cathodochromism) are being investigated but the erasure process presents some problems. These techniques sometimes utilize a reflective mode in which the viewing light traverses the material, is reflected by a mirror at the back surface, and re-traverses the optical medium. This cuts the thickness requirements in half with a corresponding decrease in voltage requirements and can be more convenient for writing and reading beam access. A related display device is one which depends on the mechanical distortion of a transmissive or reflective film. The stress is exerted by charge accumulation resulting from electron beam address and is being studied using both metallic films or deformable thermoplastics.

Thus it can be seen that a wide variety of materials and phenomena have been proposed for use in various applications for the storage and display of optical information. While the theoretical limits to the effect to be exploited may indicate advantages for a given display approach, the actual limitations may be dictated by the technology required for utilization of the phenomenon. These types of technology imposed limitations include:

1. Materials preparation -- the material must be obtainable conveniently in the proper physical form, e.g., the desired thickness. The requirements of crystalline perfection, orientation, purity, etc. must be economically fulfilled for the particular application.

2. Method of information write-in (and readout in some cases although generally it would be optically viewed). The write-in could be purely electrical, applying suitable fields employing some type of (matrix) electrode array, production of which would require small scale

fabrication technology. The use of optical or electron beam addressing would require not only beam control but photoconductor and/or electrode fabrication compatibility problems can occur with various materials combinations and processing stages.

3. Additional fabrication technology would be required, not only for points 1 and 2 but for additional device operational requirements such as optical polarization, voltage control, heating or cooling and atmospheric control. Only when the technology associated with these various considerations have been reasonably optimized can a final evaluation of device capability be reliably made. Thus although many new display structures are under active investigation, it has yet to be shown that a viable pictorial display device has been produced.

## II. STATUS OF FERROELECTRIC DISPLAYS

### II.1 Introduction

A ferroelectric material can be defined as one in which a permanent electrical polarization can be induced whose orientation can be changed by the application of an appropriate electric field. The term "Ferroelectric Display" in the present context is meant to include devices in which the active optical element is a ferroelectric material whose transparency in a given region (in some cases in combination with crossed polarizers) can be varied by electrical control of the polarization. Thus it does not include devices such as the ELF<sup>(1,2)</sup> in which the unique electrical properties of ferroelectrics (F) are exploited to supply and control the operation of electroluminescent (EL) elements.

While many ferroelectric materials have been discovered, they generally are of limited interest for display applications because they involve 180° polarization switching with little or no associated optical change. However, recently the situation has changed with the discovery of the unique electro-optic properties of several ferroelectric materials. Before considering the details of the various possible ferroelectrics, it may be of interest to discuss some general characteristics which may be expected. These will vary to some extent with the materials and structure employed but can be divided from a display application point of view as being either good, questionable, or poor.

A major advantage of a ferroelectric display is that it would be expected to be non-volatile. Since the optical state is determined

by the polarization state, which changes only by application of the appropriate electric field, loss of electrical power would have no influence on the stored information. This property in conjunction with others has also led to the study of ferroelectrics for optical memory applications.<sup>(3,4)</sup> Another valuable characteristic is that bismuth titanate in particular, and other ferroelectrics to a lesser extent, exhibit an effective threshold field effect,<sup>(5,6)</sup> a critical field magnitude must be exceeded before an applied field switches the polarization. This results in a low sensitivity to any stray fields which may be present and, of critical importance, to disturb pulses which would be required for a matrix address mode. The thermal stability for ferroelectrics should be good since little loss of stored charge would be expected to occur until the Curie temperature at which ferroelectricity is lost was approached. For the materials under consideration the Curie temperatures lie in the range 150 to 675°C. The optical contrast ratios are generally reported both for ceramic and single-crystal ferroelectrics to be 100 or more and most of the particular materials to be discussed possess a gray scale capability.

Ferroelectrics do not generate their own light, which is a disadvantage for some applications. However, since an external light source is used for viewing, the brightness attainable is limited only by the light power available and by the heating effects it would generate. The resolution which can be achieved will depend on the configuration employed, particularly the addressing process, and remains to be determined in a practical situation. The potential capabilities

have been shown to lie in the 1-2 micron range for bismuth titanate using electron beam addressing<sup>(7)</sup> and 25  $\mu\text{m}$  in doped PZT using discrete electrodes.<sup>(8)</sup> The basic switching speed should be adequate, being generally in the microsecond range, but in a display structure will be limited by the voltage which can be applied.

Two characteristics can be anticipated to present particular difficulties when consideration is given to practical display applications of ferroelectrics; materials preparation and voltage requirements. Most of the ferroelectrics of interest exhibit their unique properties only when utilized in the form of single crystals. Thus, techniques must be developed to produce quantities of uniform, high quality crystals. The one exception to the crystal requirement, PLZT ceramic, uses a hot pressing preparative method for control of grain size and uniformity, which cannot yet be termed a routine commercial process.

The voltage levels needed for operation of a ferroelectric display can be high. The exact magnitude depends on the material and configuration but, as an example, a 100  $\mu\text{m}$  thick wafer of PLZT could need a poling field of 20 kV/cm thus requiring 200 volts. Other situations could lead to lower or higher voltage requirements, which although achievable, will require careful attention.

In summary, ferroelectric materials have attracted attention for display applications because of their non-volatility, threshold switching field, good contrast and gray scale, thermal stability, high light levels, with adequate speed and resolution. Whether these properties can be realized within the constraints imposed by an actual display system is a question which remains to be answered.

## II.2 Single Crystal Ferroelectrics

With one exception, to be discussed in the next section, the ferroelectrics of particular interest would be utilized in single-crystal form. The most advanced development studies have been made on devices utilizing potassium dideuterium phosphate ( $KD_2P$ ). Various groups<sup>(9,10,11)</sup> have reported on systems generally directed toward development of very large area, real time, TV projection systems. They are based on the Pockels longitudinal electro-optic effect in which birefringence is induced by application of an electric field. The birefringence results in a differential retardation of the vibration components of incident light and thus a variable transmission through crossed polarizers. Electron beam addressing is used and generally a reflection mode to permit convenient access of the electron and light beams and the crystal cooling which is required (in contrast to the other materials to be discussed). Contrast ratios greater than 50/1, gray scale, TV rates, and resolution of up to 400 l/in have been demonstrated. Considerable difficulty has been reported in obtaining large crystal areas with uniform properties.

The unique electro-optic switching properties of bismuth titanate,  $Bi_4Ti_3O_{12}$ , have been proposed for use in display devices.<sup>(12)</sup> Bismuth titanate crystals are commonly grown from a bismuth oxide flux and possess a plate-like habit. The symmetry is monoclinic with the principal crystallographic axes essentially orthogonal, and the c-axis lying perpendicular to the large face of the crystal. The polarization direction lies in the a-c plane at an angle of approximately

four degrees to the a-axis. This results in two independently reversible components of polarization parallel to the a- and c-axes respectively. The resultant value of  $P_s$  is large ( $50 \mu\text{C}/\text{cm}^2$ ), but switching by fields along the c-axis involves the reversal of a small ( $\sim 4 \mu\text{C}/\text{cm}^2$ ) component.<sup>(13)</sup> This switching occurs at a well-defined threshold field of between 3 and 4 kV/cm, the existing remanent condition being effectively stable at fields lower than this.<sup>(5)</sup>

The principal axes of the optical indicatrix (i.e., axes along which extinction occurs between crossed polars) do not correspond to the crystallographic axes (Figure 1) of the structure. Rocking of the polarization  $P_s$  relative to the a-axis, through an angle of about  $8^\circ$ , produced by field reversal along the c-axis, results in a rotation of the optical indicatrix axes in the a-c plane through about 40 degrees. Essentially, this means that if the crystal is at extinction before field reversal, then after reversal its optical axes will be in a position which favors maximum light transmission. To make use of this effect in an optical display or memory system, it is necessary to use crystals that are cut parallel to the a-c plane. Unfortunately, the plate-like morphology of the crystals renders it difficult to produce a-c faces of a large area or of a shape suitable for display matrices. One solution to this problem is to "force" the crystal into a morphology favoring a large a-c face. This has been achieved recently in work at Westinghouse Research by depositing rf sputtered films of bismuth titanate epitaxially on the (110) face of  $\text{MgO}$ <sup>(14,15)</sup> and (110)  $\text{MgAl}_2\text{O}_4$ <sup>(16)</sup>.

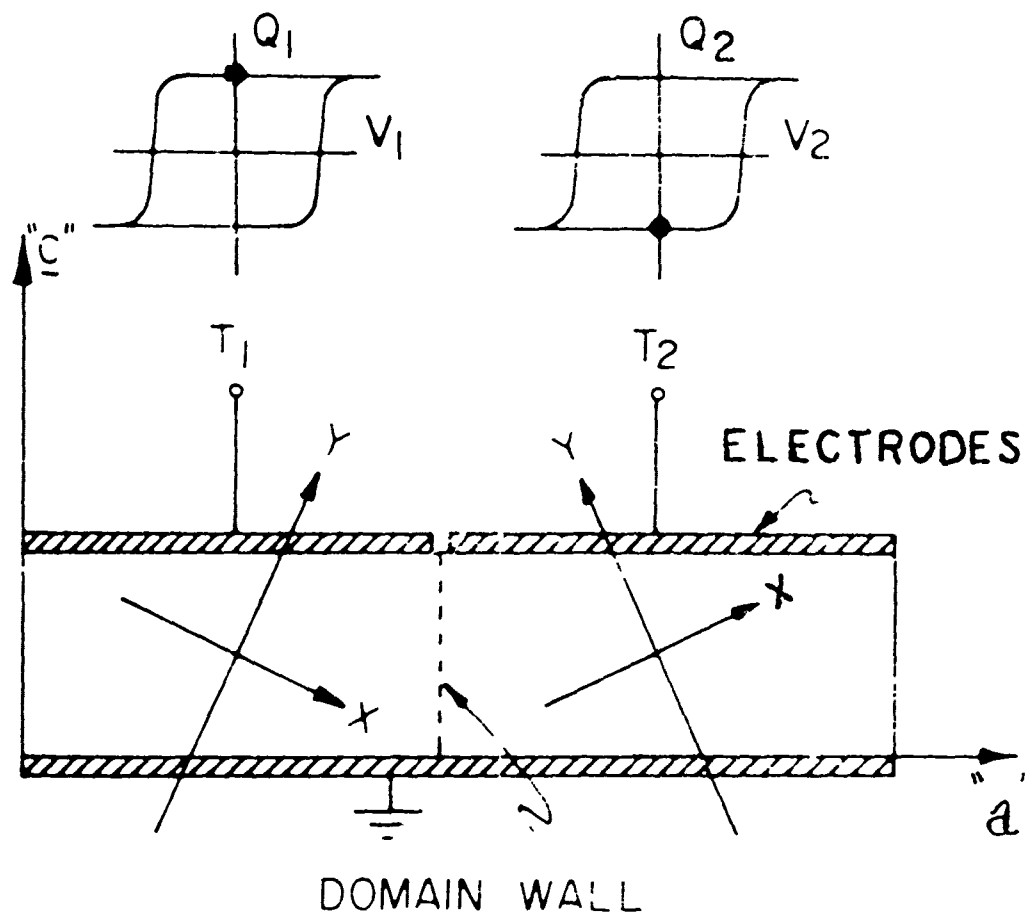


Figure 1 A  $\text{Bi}_4\text{Ti}_3\text{O}_{12}$  crystal viewed along the " $b$ " axis. The X-Y axes show the different optical indicatrix positions for opposite saturation states on the hysteresis loop. Viewing in crossed polarized light with the polarizers aligned on one of the extinction positions provides a direct nondestructive read-out of the ferroelectric polarization state [after Cummins, Ref. (12)].

An alternative approach to using bismuth titanate crystals (or c-oriented epitaxial layers) for optical display purposes is to exploit thickness contrast effects generated by birefringence differences. The method is illustrated in Figure 2 taken from recent work by S. E. Cummins and T. E. Luke<sup>(17)</sup> (Avionics Laboratory, Physics Branch, Dayton, Ohio). Two domains of opposite polarization states (referred to the c-axis) are shown, corresponding to light and dark portions of the stored image. Monochromatic light incident (at an angle  $\theta$  to the c-axis) on a given domain will be split into two vibration components in planes parallel to the principal optical axes. These axes lie in the section of the optical indicatrix corresponding to the plane of view. The birefringence  $\Delta n$  (or difference in refractive index for these axes) leads to a difference in the propagation velocities for the vibration components which, in turn, produces a wavelength difference and a relative phase retardation. On reaching the analyzer, the components are resolved into a common plane of vibration and are able to interfere. By adjusting the crystal thickness, the incidence angle  $\theta$ , and the wavelength of the radiation it is possible to produce complete destructive interference, i.e., a retardation of  $\lambda/2$ , and to achieve contrast ratios as high as 100:1.

An optical image may be written as a ferroelectric domain pattern in the crystal by sandwiching it between photoconductive and transparent electrode layers. The photoconductor layer, e. g., PVK (polyvinyl carbazole) or CdS, is placed directly on the polished face of the crystal and an electrode of  $\text{SnO}_2$  or semi-transparent metal such

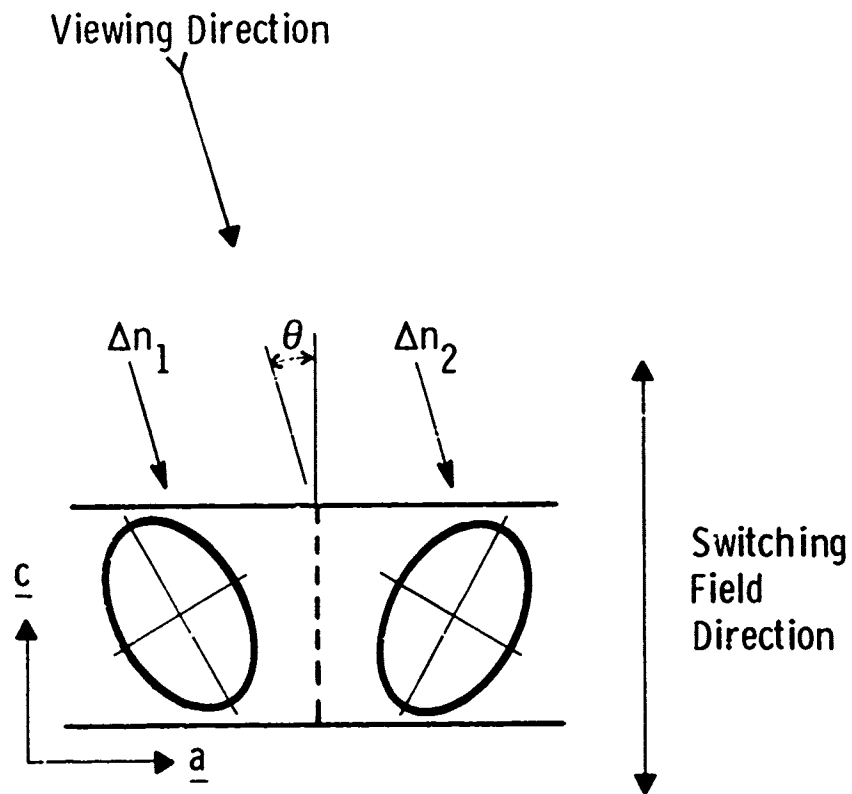


Figure 2 Arrangement for producing domain contrast by differential-retardation in bismuth titanate crystal. View of crystal is along  $b$ -axis, light is incident in the  $a$ - $c$  plane (after Cummins and Luke, Ref. 17).

as gold is applied over this. In the dark, the field across the crystal is small since the permittivity of the crystal is high compared to that of the photoconductor. Thus, when a voltage is applied between the electrode films, switching does not occur. However, when the structure is exposed to an optical image, illumination variations across the image lead to corresponding variations in photoconductor impedance, and hence to a difference in effective field across the ferroelectric. In bright areas, the field will exceed the threshold switching field and polarization reversal will occur. The stored image may be viewed under illumination conditions such as those illustrated in Figure 2. Resolutions of 90 lines/mm or higher may be achieved in this way.

Cummins and Hill<sup>(8)</sup> also showed that it is possible to write images directly into a poled crystal by scanning its surface with an electron beam. The positively charged face of the crystal is exposed to the beam and sufficient electron charge is landed to produce polarization reversal. Image resolution of 2 microns has been achieved in this manner.

A real-time display utilizing bismuth titanate has not been reported as yet. Taylor and Miller<sup>(18)</sup> concluded from a feasibility study that it could be used in a matrix addressed mode at TV rates. This study used sectioned bulk crystal plates and the conclusions were made before it had been reported that epitaxial (010) films could be prepared. Since they calculated that the optimum thickness in the b axis dimension would be 23  $\mu\text{m}$ , film growth techniques are ideally suited to prepare samples of this thickness and large dimensions in the a-c plane.

Recently two new ferroelectric materials have been proposed for use in optical devices. Gadolinium molybdate,  $\text{Gd}_2(\text{MoO}_4)_3$ , has among several unique properties the feature that the orientation of the optical fast and slow axis interchange in conjunction with ferroelectric polarization reversal.<sup>(19,20)</sup> Thus two quarter wave plates could be used, one fixed and the other of gadolinium molybdate which would provide either positive or negative  $\lambda/4$  retardation. The resultant effect could thus give a controllable net zero or  $\lambda/2$  retardation to provide transmission or extinction between crossed polarizers. Suitable large high quality single crystals can be grown<sup>(21,22)</sup> but the switching time is rather slow, values near the millisecond range being reported.<sup>(20,22)</sup> Another interesting new ferroelectric material is lead germanate,  $\text{Pb}_5\text{Ge}_3\text{O}_{11}$ .<sup>(23)</sup> Of particular interest is the fact that it is optically active with the direction of optical rotation reversible with reverse of the ferroelectric polarization.<sup>(24)</sup> This would suggest the possibility of unique optical structures but basic material properties of interest for these applications have yet to be reported.

### II.3 Polycrystalline Ferroelectrics

The one non-single crystal ferroelectric of interest for display applications is hot-pressed, ceramic, bismuth or particularly lanthanum modified lead zirconate titanate (PLZT). The use of the transparent PLZT ceramics is based on optical destructive interference arising from the birefringence which Land and associates discovered<sup>(8,25)</sup> could be introduced by poling in fine grained material. Thus it is similar to bismuth titanate being employed in the birefringence mode

described above. However, there are significant differences. The fact that polycrystalline ceramics can be used removed the requirement that certain crystallographic orientations be maintained. The magnitude of the birefringence depends on the magnitude of the remanent polarization.<sup>(26)</sup> Thus the optical retardation can be varied continuously (between certain limits), permitting selective color absorption if white light is used for read-out and grey-scale capabilities for monochromatic light in certain device configurations. The lack of squareness in the hysteresis loops of this ceramic which permits this convenient adjustment of the remanent polarization is also a disadvantage, however, in that it leads to a lack of stability toward disturb pulses.

All of the display feasibility studies reported thus far have been made using hot-pressed PZT ceramic plates which have been thinned to  $\sim 50\mu$  by lapping and polishing techniques. Land and associates investigated the device potential of the material using discrete metallic electrodes not only for poling but for the controlled variation of the polarization.<sup>(8)</sup> This permits the use of high fields and currents, and the essentially ideal switching conditions result in high contrast ratios and rapid switching speeds. Contrast ratios of up to 1000 to 1 and switching speeds of better than 100 microseconds have been reported. Information storage could be achieved by an array of discrete electrode sets with either individual or matrix addressing, although the latter could have disturb pulse difficulties. However, in order to take advantage of the potential of the material, particularly for compatibility with optical display systems and optimum resolution,

a continuous technique would seem to be more suitable instead of a discrete addressing system. Such a technique has been employed by Meitzler et al.,<sup>(27)</sup> one of the configurations employed is shown in Figure 3. For light perpendicular to the surface, maximum birefringence is obtained for a vertical polarization and zero birefringence for a horizontal polarization. Initially, PZT is poled vertically by use of the erase electrodes which consist of an interdigitated array connected so that the polarity is as indicated. "Write-in" is accomplished as described above for bismuth titanate by illuminating the appropriate regions of the photoconductor while a potential is applied across the transparent electrodes. The areas to be illuminated may be determined either by placing a photographic negative in front of the device or by scanning with a modulated laser beam. The information has thus been "written-in" in the form of a variation in polarization and therefore a variation in birefringence across the device area. It can be read-out as described above by viewing with polarized light and utilizing the phase retardation of the light. The device has the disadvantage that the areas covered by the erase electrodes are in variant bands across the image. This has been overcome by a modification called "strain-biasing".<sup>(28)</sup> The device is as illustrated, except that no erase electrodes are present, and it is mounted in a permanently bent state. The tension ( $\sim$  horizontal) direction in the ceramic becomes the "easy" direction for the polarization. Thus while the "write" operation is performed as before by using a relatively high potential across the transparent electrodes, the "erase" is performed by flooding the entire photoconductor area while applying only a moderate reverse potential.

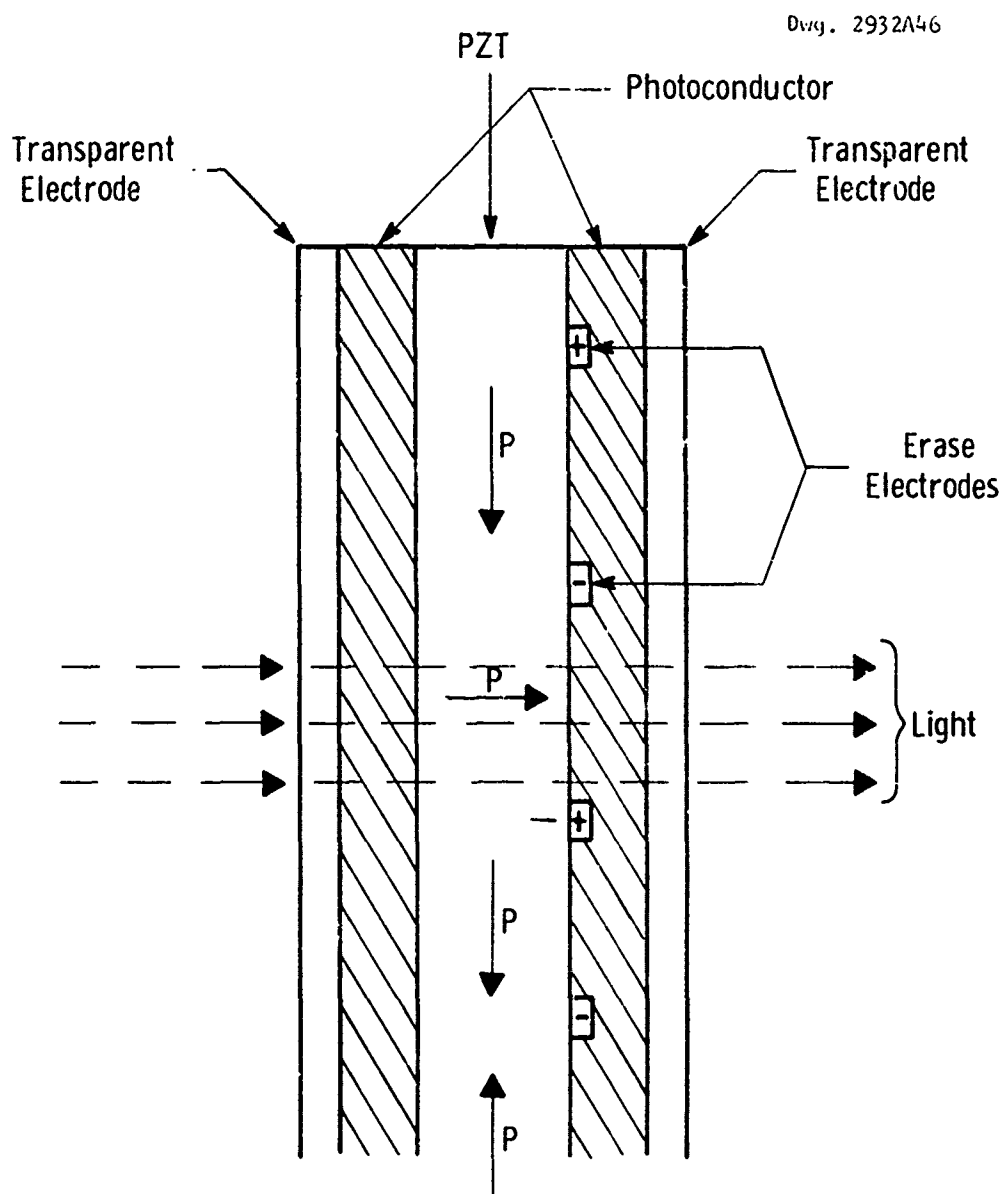


Figure 3 Portion of configuration used by Meitzler et al.<sup>(27)</sup> for PZT optical display device.

Recently, Smith and Land<sup>(29)</sup> have described a new display mode utilizing coarse grained PLZT. The longitudinal electro-optic scattering effect is used in which the amount of light scattering can be controlled by variation of the ferroelectric polarization. Using a ferroelectric photoconductor structure, negative storage with 40 line pair/mm and reasonable contrast and gray scale have been demonstrated.

### III. AIMS OF PRESENT STUDY

Although considerable advances have been made towards selecting and perfecting ferroelectric materials such as single-crystal KDP and  $\text{Bi}_4\text{Ti}_3\text{O}_{12}$  and polycrystalline PLZT for experimental display systems, further work is still required on the development of both the optimum ferroelectric medium for a practical display and on peripheral materials needed for optical, electrical or electron-beam address. Rapid progress towards a working device structure has been impeded not only by the intrinsic shortcomings of the materials themselves, but also by the large number of alternative approaches available for the final design concept. From the introductory discussion given here of the status of displays in general and ferroelectric displays in particular, it is clear that once the decision is made concerning the selection of the ferroelectric material to be used, several choices are now available for the mode of address. Final selection of the address mode is not yet feasible since rapid progress is still being made in each of the three main address approaches indicated above. In the present program we have tried to place emphasis on the use of those ferroelectric materials and address modes which offer the best prospect of testing the feasibility of the ferroelectric light valve approach for high-brightness displays.

Specifically, the aim of this research program was to develop relatively large-area display structures (5 x 7 in.) which could function in solid state real-time aircraft instrumentation systems. The program has benefited from parallel studies in these Laboratories, pursued since 1968 under Air Force Avionics Laboratory Contracts (F33615-69-C-1214 and F33615-70-C-1086), which have led to the successful growth of

hetero-epitaxial bismuth titanate films possessing electrical and optical properties closely approximating those of bulk crystals. Several technically related projects in the areas of vidicon and eibcon solid state technology and in solid state Eidophor projection systems are also being pursued in the Device Physics Department of the Laboratories. The facilities and research results generated in these projects are directly applicable and available to ferroelectric display device approaches outlined here. For convenience the program was divided into four phases: (1) optimization of ferroelectric material; (2) design and preparation of experimental, light-valve type, display devices; (3) evaluation of display characteristics with optical address and (4) evaluation of matrix electrode address. The details of these phases are given in the following sections.

### III.1 Optimization of Ferroelectric Material

The materials selected for use in this program were epitaxial bismuth titanate films, and transparent, high-density, PLZT (lead-zirconate-titanate with lanthanum oxide additives) ceramics. The epitaxial bismuth titanate samples are being prepared in these laboratories while the PLZT ceramics were obtained from commercial sources. Neither of the ferroelectric media available for the investigation had been completely optimized for display purposes. In the case of the epitaxial layers of bismuth titanate, further work was required to eliminate twinning and develop low coercive field properties. For PLZT the initial problem was to locate and evaluate commercial material with electro-optic characteristics comparable to those obtained with the Sandia processed fine-grained material. During the course of the contract the light-scattering

display mode of operation for coarse-grained PLZT was reported, and the advantages for this mode prompted a change in the emphasis of our program towards coarse-grained (4-8  $\mu\text{m}$ ) rather than fine-grained ( $\sim 2\mu\text{m}$ ) material.

### III.2 Design and Preparation of Experimental Display Devices

Several possible display structures were considered in the early stages of the program. These included simple test devices on PLZT fitted with transparent electrodes to permit the application of fields parallel and perpendicular to the surface, photoconductor sandwich structures for light address, strain biasing arrangements and interdigitated and matrix electrode structures on PLZT and bismuth titanate epitaxial films. Many of the complete device structures envisaged were predicated upon the immediate availability of optimized ferroelectric PLZT and photoconductive material. However, it soon became clear that considerable development was still needed before such materials suitable for high contrast displays would be obtained. Thus, the emphasis was changed towards simpler test vehicles to enable evaluation of materials parameters.

### III.3 Display Characteristics with Optical Address

Optical address is an attractive technique for information input since the structure required is simple, a ferroelectric and photoconductor layer sandwiched between two transparent electrodes. However, as information was accumulated as noted above, it became apparent that the shortcomings of the ferroelectric and photoconductors would

particularly handicap this approach. Also while testing could be performed using images obtained by projecting through a photographic negative, an actual real-time display device would require the availability of a scanning, modulated light beam. The situation with regard to the development of such a light source is far from clear but it could cause a major delay in the final utilization of the optical addressing mode. Thus it was decided to concentrate primary attention on the matrix approach.

#### III.4 Matrix Electrode Address

As discussed above, major emphasis has been placed on the matrix electrode addressing mode. While more complex structurally, than the optical mode, the materials requirements were as stringent and the fabrication technology required for electrode delineation were readily available in our solid state devices processing facilities. It was also anticipated that it would be possible to embody many of the fabrication aspects of the thin film transistor-electroluminescent panel (particularly the transparent thin film drive circuitry and possibly the thin film transistor circuit) being developed under a concurrent ONR Contract N00014-71-C-0268 in these Laboratories.

Various discrete electrode structures as described in Section III.2 were evaluated with initial emphasis placed on maximum contrast ratios, grey-scale capability and voltage requirements. Concentration on these basic materials parameters was dictated by the materials limitations as described in Section III.1.

#### IV. MATERIALS STUDIES

##### IV.1 Introduction -- Material Parameter Requirements

As has been described in Section III, the aim of the present program is to develop optical projection and/or large-area panel structures (5 x 7 in.) which can function in solid-state real time aircraft instrumentation systems. Two ferroelectric materials, viz., transparent hot-pressed lead-zirconate-titanate ceramics of approximately 65/35 composition doped with lanthanum (PLZT), and epitaxial bismuth titanate films were studied. Two approaches, one with optical address and one with matrix address, were chosen in this study for writing, reading and erasing the display information. In this section we will describe the requirements on material properties for these two approaches first. The fabrication processes and the results of measurements on these material properties will next be considered.

To permit optical address, the display device is fabricated as a sandwich structure which consists of a ferroelectric material, a photoconductive layer and a top and a bottom transparent (e.g., tin-doped indium oxide) or semi-transparent (gold) layers. The schematic diagram of the device structure is shown in Fig. 4. As indicated in Section II, the use of the photoconductive layer in conjunction with the ferroelectric permits selective switching of the ferroelectric in areas which are illuminated. This results in a local alteration in the polarization direction of the ferroelectric and hence in the change of birefringence (differential phase retardation mode), light scattering properties (scattering mode) or the rotation of the optical indicatrix (extinction mode).

Dwg. 6176A62

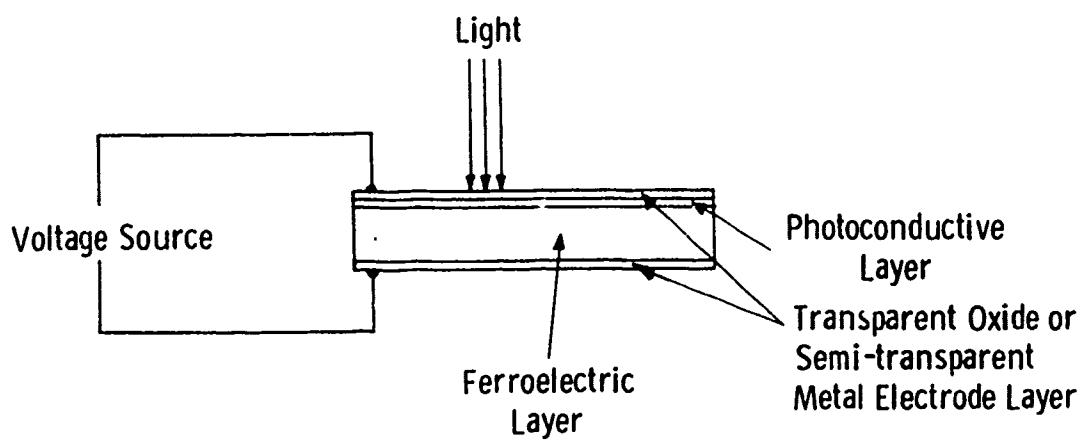


Figure 4 Schematic diagram of the PC-FE device structure.

Ideally the device will be operated as follows: In the dark when a WRITE voltage is applied to the structure, nearly all of the voltage will be applied across the photoconductor, that is,  $\frac{V_P}{V_F} \approx 10$ . Hence the ferroelectric will not switch. The criterion is, initially

$$\frac{V_P(0)}{V_F(0)} = \frac{C_F}{C_P} = \frac{\epsilon_F d_P}{\epsilon_P d_F} \geq 10$$

where C is capacitance,  $\epsilon$  is dielectric constant and d is thickness. The subscript P stands for photoconductor and F for ferroelectric. This relation requires the thickness ratio to be

$$\frac{d_P}{d_F} \approx 10 \left( \frac{\epsilon_P}{\epsilon_F} \right) \quad (1)$$

Eventually the WRITE voltage will be divided by the resistance ratio, that is

$$\frac{V_P(\infty)}{V_F(\infty)} = \frac{R_P}{R_F} = \frac{\rho_P d_P}{\rho_F d_F} \geq 10$$

This relation gives

$$\frac{\rho_P}{\rho_F} \geq 10 \left( \frac{d_F}{d_P} \right) \quad (2)$$

where R is resistance and  $\rho$  is resistivity.

When the structure is exposed to a light image, illumination variations across the image lead to corresponding variations in photoconductor impedance which gives to a difference in effective field

across the ferroelectric layer. If the field exceeds the threshold switching field of the ferroelectric, the ferroelectric will be switched. The criterion now requires

$$\frac{R_{FL} V}{R_{PL} + R_{FL}} > V_C \quad \text{or} \quad (3)$$

$$\frac{\rho_{FL} \cdot d_F}{\rho_{PL} \cdot d_P} > \frac{V_C}{V - V_C}$$

where  $V$  is the applied voltage and  $V_C$  is the coercive voltage, and the subscript  $L$  stands for condition under illumination.

In general, the device will not be operated by a dc voltage source as discussed above. If, instead of dc, a pulsed source is used, we have to take the switching speed of the device into account when we are considering an appropriate photoconductive material. Let us assume the ferroelectric itself switches within  $t_o$  at a voltage  $V_o$ , (determined from ferroelectric current transient experiments). Then the relation between the required switching time of the device,  $t_s$ , the switching time of the ferroelectric  $t_o$  and the  $R_{PL} \cdot C_{FL}$  time constant has to satisfy, to the first order approximation,

$$2.3 R_{PL} C_{FL} < (t_s - t_o) \quad \text{or} \quad (4)$$

$$\rho_{PL} \cdot d_P < \frac{.4 (T_s - t_o) d_F}{\epsilon_{FL}}$$

Here, we neglect the parameters of the transparent electrodes. If a pulsed light arrangement is used, the other parameter -- photoconductor response time, also needs to be considered.

In matrix addressing, the requirements on material parameters are less stringent than in optical addressing. The sheet resistance of the transparent (or semi-transparent) layer has to be lower than  $100 \Omega/\square$ . A requirement for the light-addressed mode is that these layers must form an ohmic contact with the photoconductive layer.

#### IV.2 PLZT Ferroelectric Ceramics

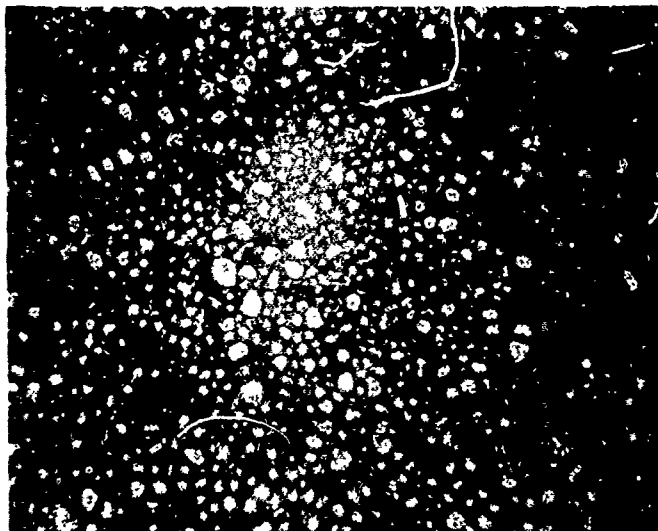
The ferroelectric ceramics studied were hot-pressed (rhombohedral) lead zirconate titanate doped with lanthanum (PLZT). The composition was 65% zirconate and 35% titanate with 7-8 at. percent lanthanum. They were supplied from two commercial sources: Vernitron and Honeywell. The electro-optic properties of these ceramics depend on the nominal grain diameter. For grain size smaller than 2 microns, described as fine-grained ceramics, they are birefringent. They exhibit orthotropic symmetry with respect to the ceramic polar axis. The effective birefringence depends on the applied electric field. Hence, the retardation of a ceramic plate can be controlled by incrementally varying the switching field. These fine-grained ceramics were used in the study utilizing the differential phase retardation mode.

For grain size larger than 2 microns, the ceramics will depolarize transmitted light by multiple internal scattering. The light scattering properties depend on the orientation of the ceramic polar

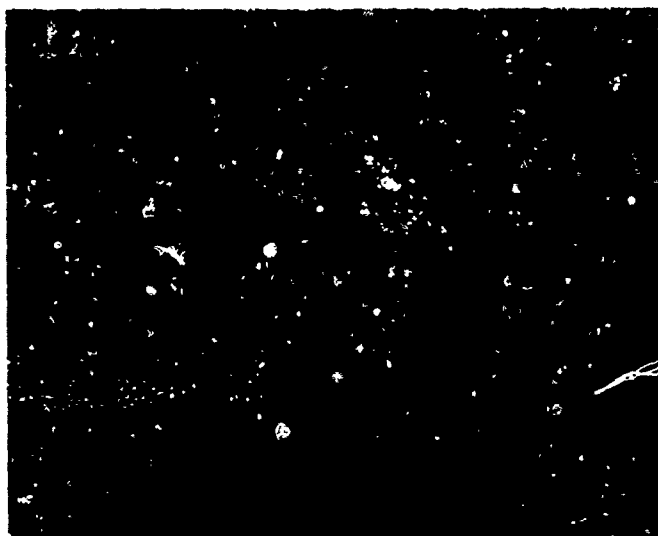
axis or the direction of electrical poling. These ceramics, called coarse-grained ceramics, were used in the study utilizing the longitudinal electro-optic scattering effect.

The PLZT ceramics after being received were mechanically lapped and polished to an optical finish. For fine-grained ceramics the thickness of the plates were controlled so as to give a half-wavelength retardation change in the differential phase retardation mode when the polarization was switched from in the plane to perpendicular to the plane. It ranged from 25  $\mu\text{m}$  to 75  $\mu\text{m}$ . For coarse-grained ceramics, the thicknesses were adjusted to give a best ON/OFF contrast ratio with still a reasonably good light transmission in the ON state, except for the study of contrast ratio versus the ceramic plate thickness. In the latter case, the thicknesses were from 100 microns to 300 microns. They were then annealed in air at 700°C for one hour which reduced any mechanical damage and relieved any strain induced during previous sample preparation processes. Some specimens were thermally etched at 1300°C in a protective lead oxide-rich atmosphere to study the grain size.

Figure 5 shows etched microstructures of fine-grained PLZT ceramics (a) Vernitron materials and (b) Honeywell material. The grain size is not uniform. It ranges from 1  $\mu\text{m}$  to 3  $\mu\text{m}$ . The grains are not densely packed. At the grain boundaries there may be many residual pores or voids left behind by the more volatile lead oxide which vaporizes during thermal etching. Figure 6 shows etched microstructures of coarse-grained PLZT ceramics. (a) early Honeywell

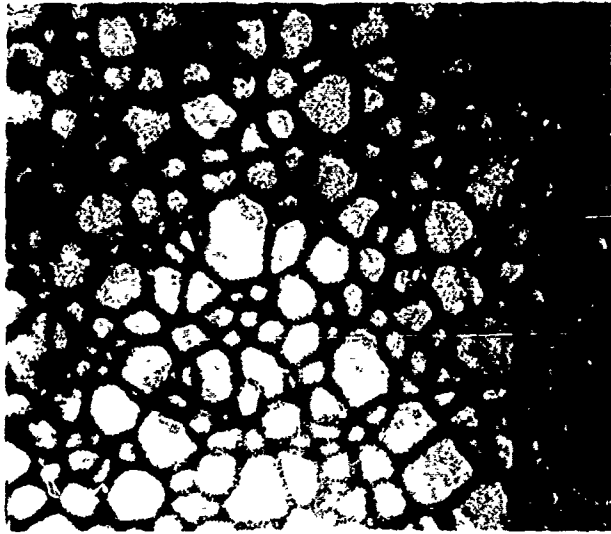


(a)

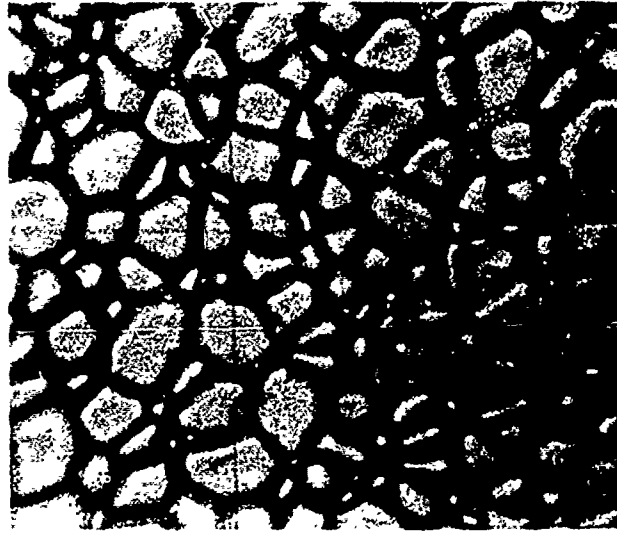


(b)

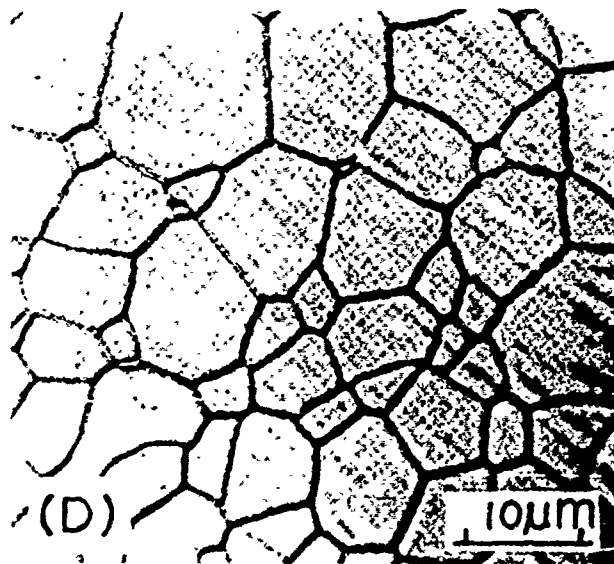
Figure 5 Etched microstructures of fine-grained PLZT ceramics.  
(a) Vernitron material and (b) Honeywell material.



(a)



(b)



(c)

Figure 6 Etched microstructures of coarse-grained PLZT ceramics. (a) early Honeywell material, (b) latest Honeywell material, and (c) Sandia material. (30)

material, (b) latest Honeywell material and (c) Sandia material.<sup>(30)</sup>

The average grain size of Honeywell material is about 4-5  $\mu\text{m}$ , while that of Sandia is about 10  $\mu\text{m}$ .

The resistivity of PLZT ceramics was measured. It was about  $10^{11} \sim 10^{12} \Omega\text{-cm}$ . The ferroelectric hysteretic and polarization switching studies were made with a modified Sawyer and Tower bridge circuit.<sup>(31)</sup> Fields were applied perpendicular to the plane of the ceramic plates with gold electrodes deposited on both surfaces. The typical saturation polarization and the remanent polarization of Vernitron fine-grained ceramics were  $55 \mu\text{C}/\text{cm}^2$  and  $33 \mu\text{C}/\text{cm}^2$ , respectively. The coercive field was 7.4 kV/cm. These of Honeywell fine-grained ceramics were  $50 \mu\text{C}/\text{cm}^2$  and  $38 \mu\text{C}/\text{cm}^2$ , respectively. The coercive field was 4.5 kV/cm. The typical saturation coarse-grained ceramics were  $52 \mu\text{C}/\text{cm}^2$  and  $50 \mu\text{C}/\text{cm}^2$ , respectively, and the coercive field was 5.6 kV/cm. These data seemed higher than those of Haertling et al.<sup>(32)</sup> These ceramics had essentially square hysteresis loops, as shown in Fig. 7. The squareness (ratio of remnant to saturation polarization) of the loop was about 0.96. The effects of temperature on the hysteresis loop were also studied. The results were similar to those observed by Haertling.<sup>(30)</sup> The remanent polarization and the coercive field gradually decreased with increasing temperature. No abrupt change in polarization was observed at the Curie point.

The dielectric constant and the dissipation factor of virgin ceramics (not previously electrically poled) were evaluated by measuring the capacitance and the conductance, using Boonton bridges, Model 75C,



Figure 7 Hysteresis loop observed on latest Honeywell coarse-grained ceramics. Scale: vertical,  $20 \mu\text{C}/\text{cm}^2$  and horizontal,  $2.35 \text{ KV}/\text{cm}$ .

for frequencies from 5 KHz to 500 KHz and model 75A-S8 for frequency at 1 MHz. The measurements were made with gold counter electrodes deposited on both surfaces. The room temperature dielectric constant ranged from 3000 to 4000 at 5 KHz, agreed with the results of Haertling et al.<sup>(30)</sup> It decreased slightly with increasing frequency. The dissipation factor was about 3 ~ 5 % at 5 KHz and increased with increasing frequency. It was interesting to note that both the dielectric constant and the dissipation factor decreased after the ceramic was subjected to a cycling electric field of  $3 E_c$ , here  $E_c$  being the coercive field. Figure 8 shows a typical room temperature dielectric constant and dissipation factor versus frequency curves measured from a fine-grained ceramic (Vernitron). The solid curves are from the virgin ceramic and the dashed curves are after being cycled with an electric field.

#### IV.3 Epitaxial Bismuth Titanate Films

The epitaxial bismuth titanate films were prepared by rf sputtering using ceramic targets containing an excess of  $\text{Bi}_2\text{O}_3$  in order to compensate for the loss of this component.<sup>(14)</sup> The target composition was  $0.8 \text{ Bi}_4\text{Ti}_3\text{O}_{12} + 0.2 \text{ Bi}_{12}\text{TiO}_{20}$ . Films were deposited at substrate temperature slightly higher than the Curie temperature which gave films of good optical quality. It was found in previous studies<sup>(14,15)</sup> that films grown on (110) MgO were twinned and multi-domain as shown in Fig. 9. The occurrence of twin pattern was attributed to the difference in the thermal expansion coefficients between the bismuth titanate, which were approximately  $6, 11$  and  $14 \times 10^{-6}/^\circ\text{C}$  along the a, b and c axes respectively<sup>(33)</sup>, and that of MgO,  $14 \times 10^{-6}/^\circ\text{C}$ . A thermal expansion

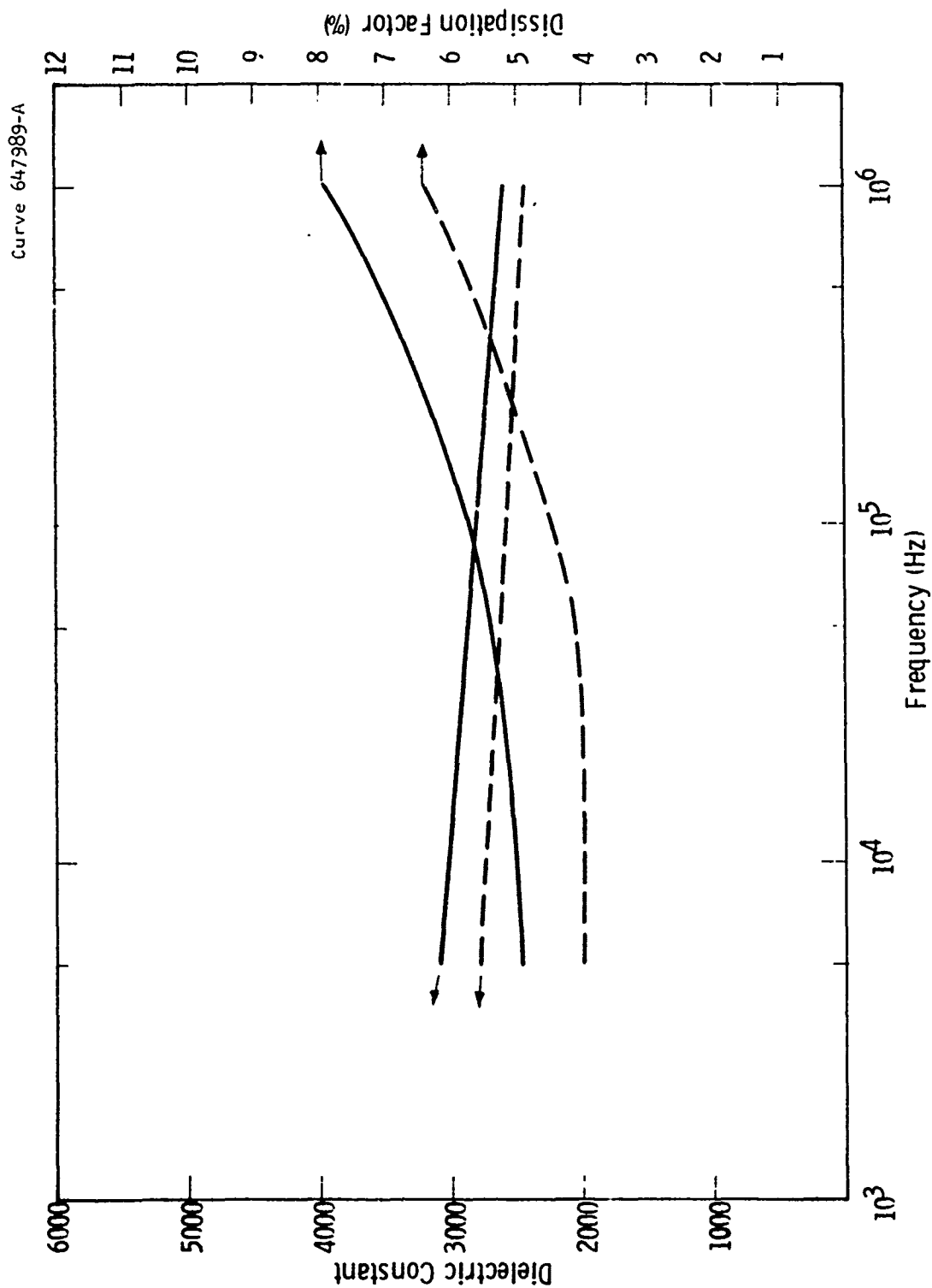


Figure 8 Dielectric constant and dissipation factor versus frequency of a 8/65/35 PLZT (Vernitron).



Figure 9 Microstructure under crossed polarizers of bismuth titanate films grown on (110) MgO. Elongated regions are a-up regions and the background is 4-up regions.

mismatch arose on cooling from the growth temperature along that axis in the film plane lying parallel to the a or b axis of the twin structure. This generated a strong compressive clamping force along this axis of the film, which presumably also contributed to the adoption of the striped twin structure on cooling below the Curie temperature. Because of the piezoelectric fields associated with this stress films grown on MgO could not be completely poled to a single-domain state unless they were detached from the substrate and annealed above the Curie temperature.<sup>(15)</sup> Thus, the substrate-attached films on (110) MgO were unsuitable for electro-optic display purposes.

To solve the above difficulty, (110) spinel ( $\text{MgAl}_2\text{O}_4$ ) crystals which possessed planes structurally similar to the (110) plane of MgO were investigated. Films grown on (110)  $\text{MgAl}_2\text{O}_4$  possessed excellent optical quality and comprised the desired single (010) orientation needed for display applications. The absence of a-b twinning in these films resulted from the lower thermal expansion coefficient of  $\text{MgAl}_2\text{O}_4$  ( $7.4 \times 10^{-6}/^\circ\text{C}$ ) compared with MgO. A tensile stress (relative to the b-axis of the titanate) generated in the film on cooling from the growth temperature favored parallelism of the large a-axis ( $a = 5.45 \text{ \AA}$ ), rather than the b axis ( $b = 5.41 \text{ \AA}$ ), with the substrate surface. Unfortunately, the relatively large thermal expansion coefficient of bismuth titanate along the c-axis<sup>(33)</sup> ( $\sim 14 \times 10^{-6}/^\circ\text{C}$ ), compared with that for  $\text{MgAl}_2\text{O}_4$ , led to cracking and peeling of films thicker than  $5 \text{ }\mu\text{m}$ . To overcome this problem, a stress compensation technique was used. This technique utilized bending stresses in the substrate

during film deposition to compensate for the c-axis tensile stress in the film. Adherent films thicker than 10  $\mu\text{m}$  were successfully grown. The cracks were not completely eliminated but they did not adversely affect the optical switching behavior of the film.

#### IV.4 Photoconductors

##### a) ZnSe

ZnSe films were fabricated essentially by standard vacuum evaporation. The system used is schematically shown in Fig. 10. The charge, consisting of pressed pellets of the pre-fired powdered materials, was slowly evaporated from a tantalum crucible and condensed on a PLZT substrate kept at 350°C. A vacuum of the order of  $10^{-5}$  torr is quite sufficient. The sticking probability on the substitute is noticeably below unity if the substrate is kept at high temperature. Hence, crucible and substrate were enclosed in a "hot chamber" (quartz) which was uniformly heated at all sides, within the evaluated bell jar. Particles (atoms, ions) of ZnSe may then bounce several times from wall to wall during evaporation before they condense into the final film. ZnSe films prepared in this way were very uniform, adhering well to glass or PLZT substrate. The thickness of the films was predetermined by a weighed amount of charge. More accurate determination of a film thickness was possible by weighing the substrate before and after evaporation, or by counting interference fringes. The resistivities of ZnSe films were measured by depositing 2  $\mu\text{m}$  thick ZnSe layers on heated glass substrates, aluminum electrodes of 23 mils by 30 mils with a gap of 10  $\mu\text{m}$  by 30 mils being used. The dark resistivity

Dwg. 853A479

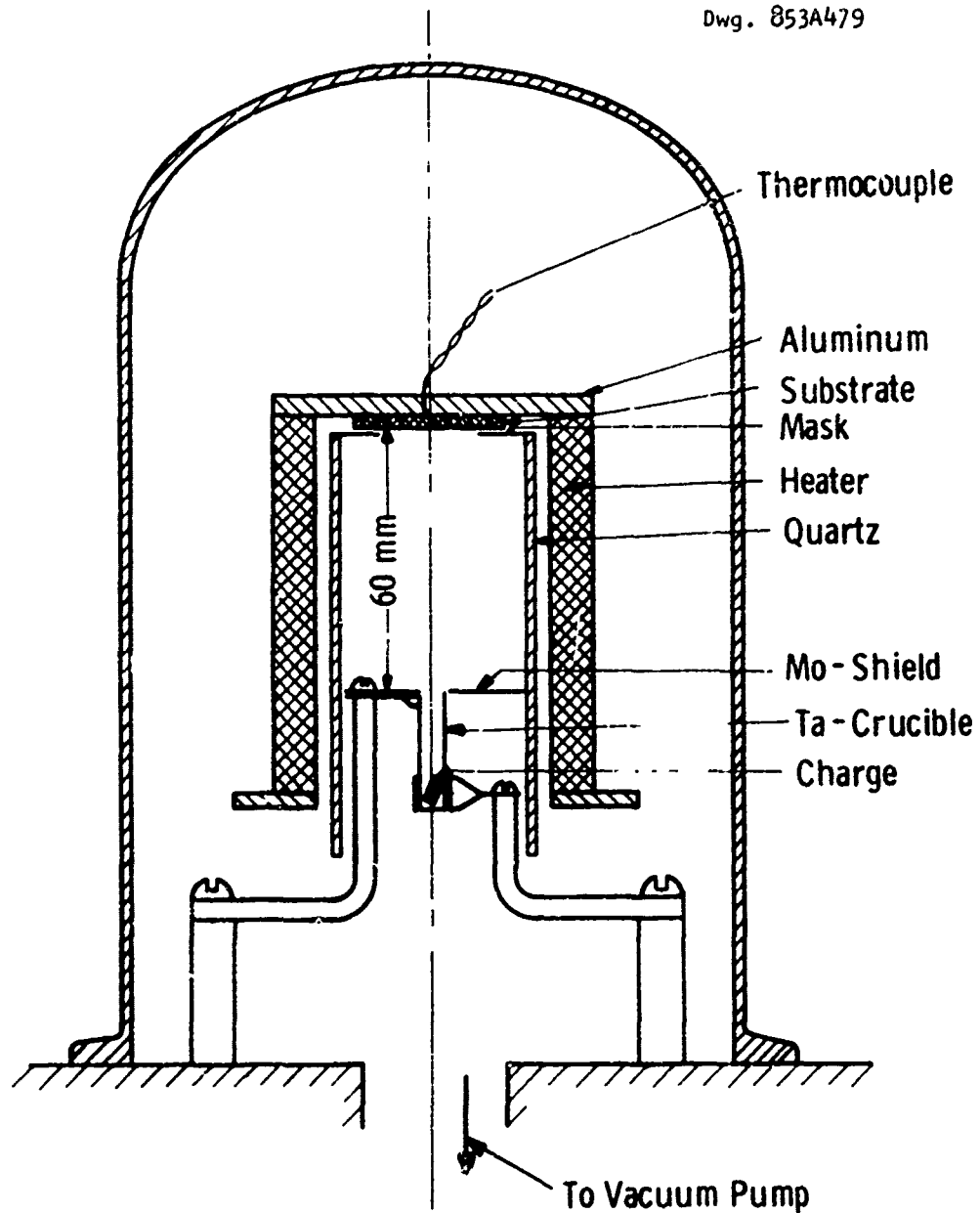


Figure 10 Scheme of vacuum evaporation within a hot chamber for ZnSe films.

was about  $7.5 \times 10^{11} \Omega\text{-cm}$ . To measure the resistivity under light illuminating condition, the sample was exposed to the light from a microscope illuminator (American Optical Company model 350) which was set at the strongest intensity position. The distance from the light bulb to the film was about 1 inch. The resistivity under the light illumination decreased to about  $5.5 \times 10^8 \Omega\text{-cm}$ , a change of about three order in magnitude.

The appearance of ZnSe films deposited on PLZT at  $350^\circ\text{C}$  were yellowish and opaque. It was suspected that some reaction might have occurred at the PLZT ceramic and ZnSe interface at this deposition temperature. To prevent this from occurring, a thin  $\text{SiO}_2$  of  $700 \text{ \AA}$  was sandwiched between the PLZT and ZnSe layer. The ZnSe then became clear and transparent with a slight yellowish color.

To study the feasibility of light modulation using ZnSe on PLZT, we deposited semitransparent gold electrodes on both major surfaces of the ZnSe/PLZT multi-structure. The hysteresis loops were examined under the dark and light conditions. Figure 11 shows typical 60 Hz hysteresis loops. The inner loop was obtained in the dark, while the outer one was under light illumination. Thus a weak photoconductor modulation using ZnSe was demonstrated. The effect, however, was too small in magnitude to be useful for display purposes. The result could be improved if a thinner  $\text{SiO}_2$  layer or a much stronger intensity light was used. This would show a better photoconductivity modulation, and the loop under the light illumination would open up much further.

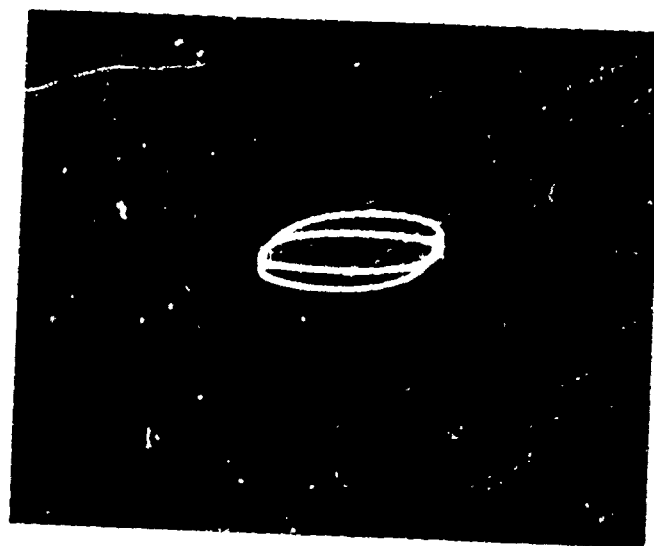


Figure 11 Typical 40 HZ hysteresis loops of ferroelectric (PLZT) - photoconductor (ZnSe) sandwiched device. Inner loop is in the dark and outer loop is under light illumination.

b) PVK

The organic photoconductor PVK, doped with 2, 4, 7-trinitro-9-fluorenone (TNF) at the ratio of 10 to 1 to make it active in the visible region of the spectrum, was mixed in a solvent of 50-50 methylene chloride and p-dioxane. The solution was mixed with the following ingredients: 8 gram polyvinyl carbazole, 0.8 gram trinitro-9-fluorenone, 30 ml methylene chloride and 30 ml p-dioxane. After mixing, the mixture was stirred and heated in a brown bottle at 55°C to 60°C for 8 hours. To coat the PVK on PLZT ceramics, the samples were dipped in the mixture and pulled out fast. This gave a uniform 3-12 micron thick coating. This procedure could be repeated to get a thicker coating. A good PVK layer of  $\sim 20 \mu\text{m}$  thick appeared to be dark brown in color and translucent. Sometimes after the sample was pulled out from the mixture, the appearance of PVK coatings would change to milky brown and lose the transparency. This appeared to be due to condensation of moisture. This tendency was corrected by drying the sample with a hot heat gun or by warming it on a hot plate. Both would bring the PVK layer back to the original brownish transparency.

The resistivity of PVK layer was measured on a sample 16.5  $\mu\text{m}$  thick. This layer was coated on a glass slide which had a predeposited aluminum layer to serve as the base electrode. A semi-transparent gold dot evaporated on the PVK was used as the upper electrode. The typical dark resistivity was about  $5.55 \times 10^8 \Omega\text{-cm}$ . The resistivity under the illuminating condition was measured by shining the incident light through the semitransparent dot electrode. Only about one order of magnitude change in resistivity was noticed.

c) CdS

The CdS films were prepared by rf sputtering from a hot pressed CdS target 5 inches in diameter and 1/4 inch in thickness. The sputtering was performed in an 18 inch bell jar in a mixing gas consisting of 98% argon and 2% hydrogen sulfide ( $H_2S$ ). The sputtering gas pressure was set at 5 mtorr. The input power was 80 watts. The film deposition rate under these conditions was 100 Å/min.

Films were first deposited on quartz substrates for resistivity and photo-sensitivity measurements. The film deposited at substrate temperatures lower than 250°C tended to peel after cooling. To obtain adherent films the substrate temperature was increased above 300°C. Films deposited at higher temperatures were highly oriented. Results on resistivity measurements on several typical films are listed in Table I. The resistivity measurements were made with indium as the contact electrodes. The electrodes were separated with a gap of 10  $\mu m$  and a width of 30 mils. The typical film thickness was about 6000 Å. The resistivity under the light illuminating condition was measured the same way as that used for ZnSe films. The annealing conditions were 450 ~ 500°C for 1 hour in air.

As shown in Table 1, the CdS dark resistivity increased with the substrate deposition temperature. For temperatures higher than 380°C, the dark resistivity, however, started decreasing. The film probably became sulfur deficient at higher substrate temperatures. The highest dark resistivity obtained was about  $1.8 \times 10^8 \Omega\text{-cm}$  on films deposited at a substrate temperature of about 370°C. The photosensitivity of as-grown films was low. The resistivity changed only three orders of magnitude under the

## TABLE I

43

illumination condition mentioned above. The Dark/Light resistivity ratio was highest, about  $2.33 \times 10^3$ , for films deposited at 370°C.

The effects of annealing on the film resistivity will be described next. The annealing was performed in a quartz tube furnace for one hour in air at about 450-500°C. The dark resistivity in general increased after annealing. For films deposited at temperatures above 380°C, which were probably slightly sulfur deficient (or cadmium-rich), the dark resistivity decreased slightly after annealing. It was assumed that the excess cadmium might be oxidized during the annealing process. The photoconductivity of the films increased considerably after annealing. The Dark/Light resistivity ratio was increased to about five orders in magnitude.

#### IV.5 Transparent Conductive Films

The transparent conductive film studied was tin-oxide doped indium oxide. The film was fabricated by rf sputtering in the same system as used to grow CdS films. The sputtering target consisted of an indium oxide ( $\text{In}_2\text{O}_3$ ) with 9 mole % tin oxide ( $\text{SnO}_2$ ), and was in the form of a hot-pressed disk with a diameter of 5 inches and a thickness of 1/4 inch. Films were deposited in a mixing gas of 50% argon and 50% oxygen at a pressure of 6  $\mu\text{m}$ . The rf power input was about 80 watts, resulting in a film deposition rate of about 45 Å/min. The substrate temperature varied from 450°C to 500°C.

It was found that the film resistivity changed with the substrate deposition temperature. The higher the temperature, the lower the film resistivity. To study the effect of substrate temperature on the film resistivity, several deposition runs were made at

different temperatures on quartz substrates. Film sheet resistances were measured with indium electrodes of 30 mils wide and a 6 mils gap. Results of room temperature resistivity versus the substrate deposition temperature is given in Fig. 12. The film resistivity was high, about 1  $\Omega$ -cm, when grown on an unheated substrate. The resistivity exponentially decreased with the increasing substrate deposition temperature. The resistivity was about  $1 \times 10^{-3}$   $\Omega$ -cm for films deposited at 500°C.

The effect of annealing in air was also investigated. The resistivity of a film deposited on a unheated substrate was decreased to  $6 \times 10^{-3}$   $\Omega$ -cm, only twice higher than that of film deposited at 450°C.

Studies were also made to develop some techniques of etching and delineating the patterns on the transparent film. Two techniques were successfully developed. The first was chemical etching with oxalic acid. The second was with the photoresist rejection method. In the first method, the transparent conductive layer was masked with a photoresist layer and then etched in concentrated oxalic acid at about 65°C. The etch rate was about 38 Å/min. Figure 13 shows an etched pattern with a 12  $\mu$ m strip line. The second method, photoresist rejection method, was as follows. A glass substrate was first covered with a positive photoresist layer. This layer was then delineated with a mask. After pattern delineation, an indium oxide transparent conductive film was deposited over the substrate. The film deposited on the patterned photoresist layer was rejected with the photoresist by agitation in an ultrasonic vibrator. A few minute rinse in a warm

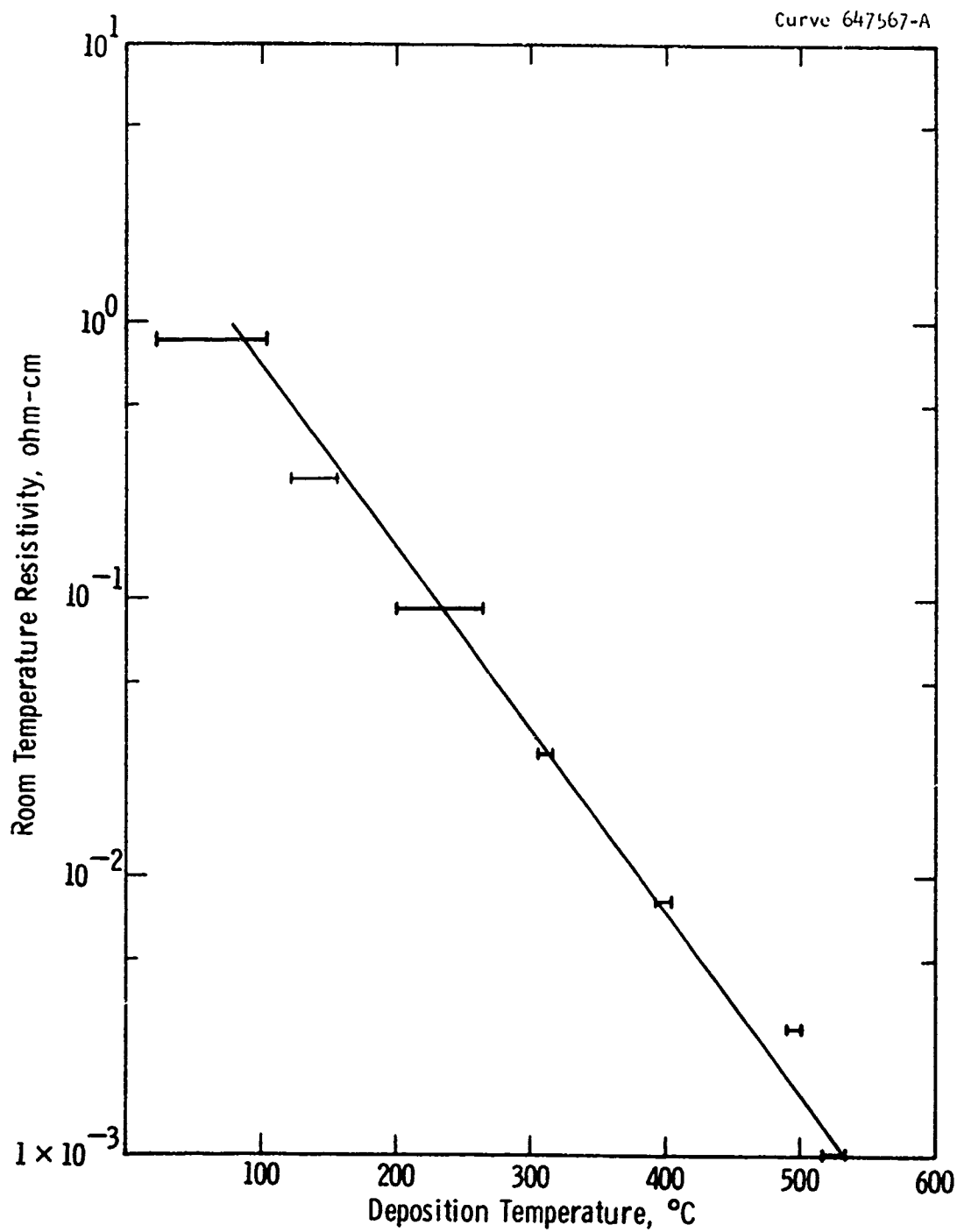


Figure 12 Room temperature resistivity of indium-oxide films versus the substrate deposition temperature.

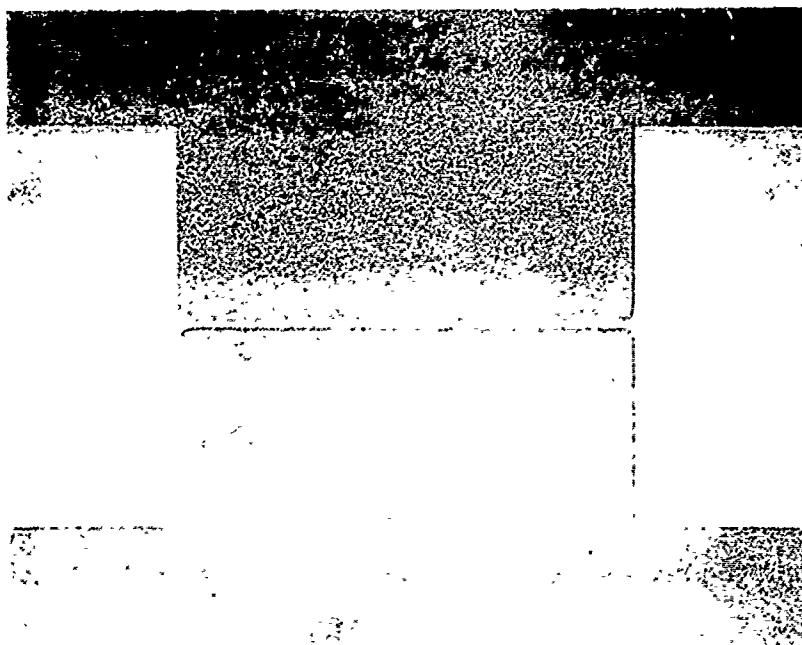


Figure 13 Delineated tin-oxide doped indium oxide pattern after being etched with oxalic acid. The width of the strip line is 12  $\mu\text{m}$ .

NaOH solution was then used to remove any residual stain left behind by the photoresist. By this technique, lines as narrow as 10  $\mu\text{m}$  were satisfactorily delineated. Figure 14 shows photos taken after the transparent conductive film was deposited on the delineated pattern. Films deposited on the photoresist were wrinkled, cracked or peeled. Films in the windows were firmly adherent to the glass substrate. Figure 15 shows a photo taken after the photoresist layer and the overlying transparent conductive film were rejected. The width of the strip line in this case is 10  $\mu\text{m}$ .

#### IV.6 Opaque GaAs and Insulating $\text{SiO}_2$ Multilayers

On PLZT display panels using the X-Y matrix addressing scheme, each active display element is surrounded by some dead areas. Light transmission through these areas interferes with the display function of active areas. To prevent this, an opaque multilayer which consisted of a 2  $\mu\text{m}$  GaAs and a 2000  $\text{\AA}$   $\text{SiO}_2$  layer was used to mask the dead areas. A 2  $\mu\text{m}$  thick amorphous GaAs layer was found to be optically dense enough to satisfy this purpose. But its resistivity was about  $3.38 \times 10^6$   $\Omega\text{-cm}$  which was several orders lower in magnitude than that of PLZT ceramics. To avoid any surface leakage via the GaAs, it was necessary to insulate this layer from the contact electrode deposited on it. This was achieved by depositing a 2000  $\text{\AA}$   $\text{SiO}_2$  layer on the opaque GaAs layer. This multilayer structure was fabricated in two separate systems as follows.

The first GaAs layer was deposited in a MRC rf sputtering system. The cathode consisted of a 5-inch diameter, 1/4 inch thick

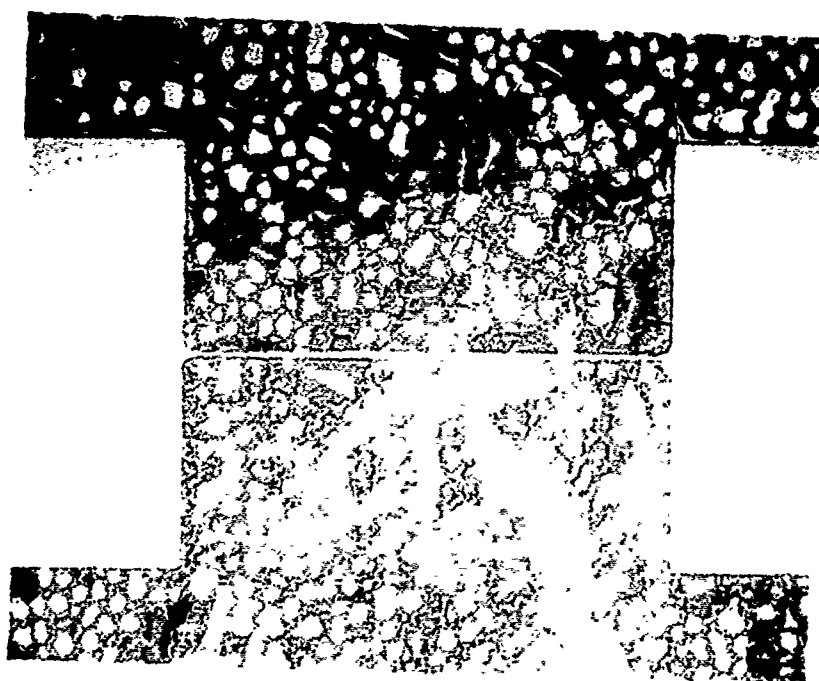
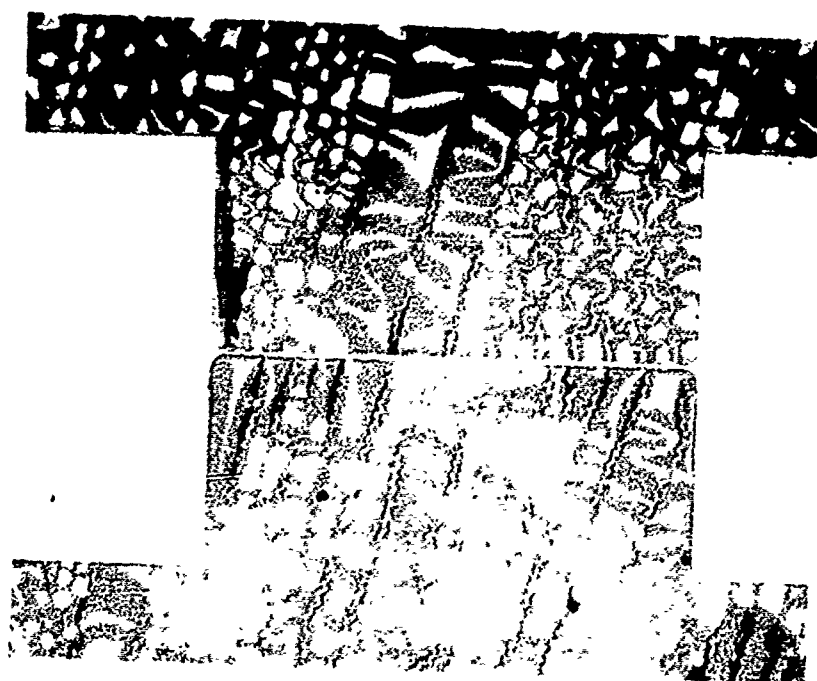


Figure 14 Photographs of tin oxide doped indium oxide films deposited on photoresist pattern.



Figure 15 Tin oxide doped indium oxide pattern delineated with rejection technique. The width of the strip line is 10  $\mu\text{m}$ .

polycrystalline GaAs target. The deposition was performed in an argon atmosphere at a gas pressure of 7  $\mu\text{m}$ . The input power was about 100 watts. The film deposition rate under these conditions was about 38  $\text{\AA}/\text{min}$ . (The growth study on GaAs films was conducted by Dr. A. J. Noreika under a Westinghouse funded research program.)

The upper  $\text{SiO}_2$  insulating layer was grown in a Varian rf sputtering system. The sputtering target was made of two 9-inch diameter semi-circular quartz disks with a thickness of 1/4 inch. The disks were mounted under the copper cathode electrode by ceramic clips around the circular periphery. Surrounding the space between the target and the substrate table was a two-turn copper coil shielded by ceramic beads. The rf field from the copper coil was used to sustain the glow discharge at low pressures. The distance between the target and the substrate was about 2.25 inch. Depositions for  $\text{SiO}_2$  layers were operated in an oxygen-argon mixing gas at a pressure of about 3  $\mu\text{m}$ . A typical input power to the cathode and the rf coil were about 2.25 in. Depositions for  $\text{SiO}_2$  layers were operated in an oxygen-argon mixing gas at a pressure of about 3  $\mu\text{m}$ . A typical input power to the cathode and the rf coil were about 300 watts and 200 watts, respectively. The deposition rate was about 120  $\text{\AA}/\text{min}$ .

After the multilayer deposition, the active regions on PLZT for display were opened by the photoresist and etching techniques. The  $\text{SiO}_2$  insulating layer was etched with a buffered HF solution and the opaque GaAs layer was with a methanol-bromine solution. In the latter solution, the bromine concentration was diluted to slow

down the etch rate. A photo showing the etched windows and the blocked dead areas is given in Fig. 16. The GaAs layer was slightly undercut for about 1 mil. The square windows of 10 mils by 10 mils on the  $\text{SiO}_2$  layer are also observable.

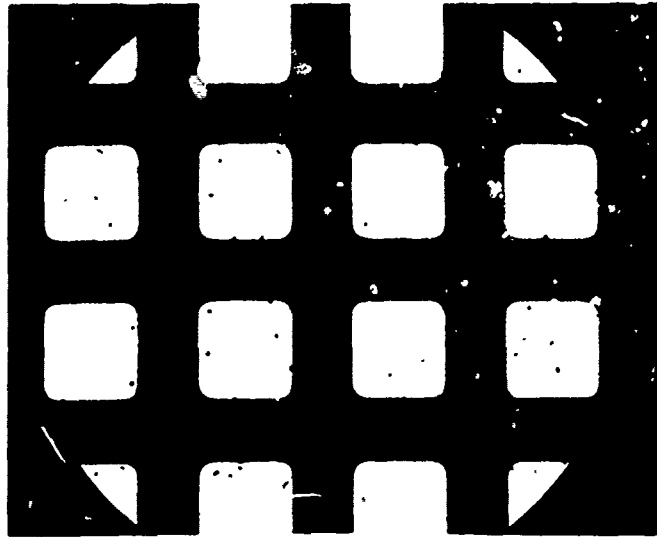


Figure 16 Photograph of PLZT windows. The dead areas are blocked with GaAs-SiO<sub>2</sub> multilayer.

## V. EVALUATION OF DISPLAY PROPERTIES

### V.1 Test Results on PLZT Fine-Grained Ceramics

Two different kinds of PLZT ceramics were tested. One was fine-grained ceramic originally proposed for use in the birefringent display mode; and the other was recently developed at Sandia for the light scattering mode. The principle of the devices using fine-grained ceramics was based on the differential phase retardation between the components of a polarized light beam. The change in effective birefringence when the polarization direction was switched from perpendicular to the ceramic plate to parallel to the plate or vice versa would produce a half-wavelength retardation. Therefore when the device was first set to a transmission (ON) state, it would be switched off if the polarization direction was changed by means of an external electric field. To observe this contrast behavior, a monochromatic light source was needed. The device was placed between crossed polarizers or parallel polarizers. A compensator was also required to compensate for the sample thickness.

#### a) Optical Address Studies

The first device tested had a photoconductor-ferroelectric sandwich structure. The upper electrode (on the photoconductor side) used a semi-transparent gold layer. The bottom electrode consisted of an array of interdigitated 1-mil fingers spaced at 1 mil, as shown in Fig. 17. The photoconductor used was CdS. Figure 18 shows a device fabricated from a 3 mil polished PLZT (Honeywell) ceramic sample and a rf sputtered 1  $\mu$ m thick CdS photoconductive layer. The polarization

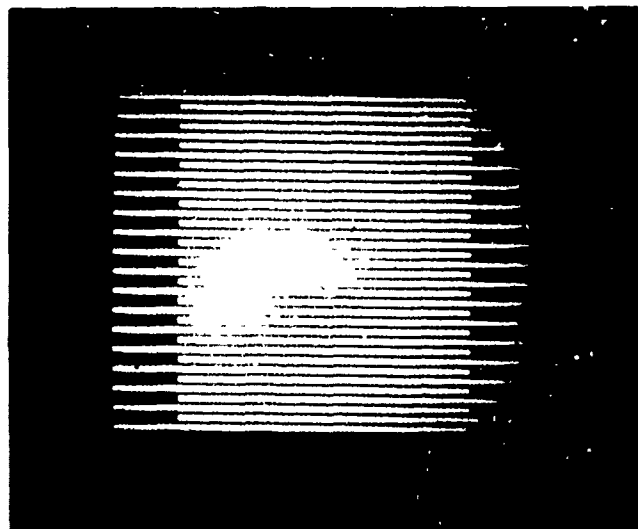


Figure 17 Interdigital finger array used for bottom switching electrodes.

of the PLZT was just poled parallel to the ceramic plane by applying a 25 kV/cm electric field between the bottom interdigital electrodes. The field was removed. A field, perpendicular to the plane, of about 5~8 kV/cm, which was slightly higher than the coercive field, was then applied between the semitransparent upper electrode and the bottom electrodes. The device was selectively illuminated. The intensity of the monochromatic light ( $\lambda = 580 \mu\text{m}$ ) was varied to modulate the CdS conductivity.

The results were not very encouraging. Difficulty was experienced in inducing switching and contrast changes in the areas selectively illuminated with light incident from the CdS coated side. The problem appeared to arise from two reasons. The first was the low dark resistivity value of the CdS (approximately  $10^8 \Omega\text{-cm}$ ), which failed to satisfy the equation (2) in Section IV. the second was poor contrast change of PLZT ceramics between ON and OFF states, apparently due to high residual porosity and large grain size of the material. To evaluate the photoconductor resistivity problem, let us reconsider some device parameters involved in Eq. (2), Section IV. If we choose a PLZT thickness of  $75 \mu\text{m}$  and a photoconductor layer  $1 \mu\text{m}$  thick, the dark resistivity of the photoconductor has to be 750 times higher than that of PLZT, about  $3.75 \times 10^{14} \Omega\text{-cm}$ , to satisfy this equation. There is no such photoconductor available at the present time. The alternative is to increase the thickness of the photoconductor. The highest dark resistivity of CdS we obtained is about  $2 \times 10^8 \Omega\text{-cm}$  which would indicate the need for a very thick CdS layer,

which is very difficult to grow. The use of other photoconductors such as ZnSe or PVK, which have a higher dark resistivity of about  $7.5 \times 10^{11}$  and  $5 \times 10^{11} \Omega\text{-cm}$  respectively, may be more promising. But even with these photoconductors, the thickness required is still very great. In view of materials limitations encountered with both the photoconductors and PLZT ceramics, the X-Y matrix address rather than the optical address approach was chosen for the later display study. It was also hoped that direct electro-optic evaluation of this type would lead more quickly to the selection of improved PLZT samples (possessing superior contrast properties) which might later be re-examined with the optical address mode.

b) Address via IDT and Matrix Electrode Structures

One of the difficulties encountered in switching the devices with the photoconductor-ferroelectric sandwich structure was very low contrast ratio arising from poor PLZT ceramics. To examine the contrast behavior of these ceramics, a simpler test device was fabricated by depositing interdigitated (IDT) finger electrodes on both ceramic surfaces. The upper and the bottom electrodes were matched exactly. The ferroelectric polarization direction was switched from parallel to the plate to perpendicular to the plate, or vice versa, with proper fields applied to the upper and the bottom electrodes. (The sample was placed between crossed polarizers.) The optical contrast changes accompanied with electrical switching were found to be poor on Honeywell's materials. The result suggested that the PLZT ceramics (Honeywell) used in early devices with the photoconductor-ferroelectric

sandwich structure might not be suitable for device applications utilizing the differential phase retardation mode. Therefore, for fine-grained PLZT ceramics we used the materials supplied from Vernitron only.

For X-Y matrix address approach, the conductive electrodes used were either semi-transparent gold electrodes or transparent tin oxide doped indium oxide electrodes. The semi-transparent gold electrodes were tried first because of the simplicity of fabrication. They were evaporated through a metal mask having 4 mils by 3/8 in windows spaced at 6 mils apart. By cross-depositing the upper and lower electrodes, 4 mils by 4 mils overlapped areas were formed. Figure 18 shows a typical sample after the electrodes were deposited. It was mounted on a 22 mm x 60 mm cover glass with transparent glycol phthalate.

To test the sample, provision was made to strain-bias<sup>(28)</sup> the ceramic, so as to provide a remanent polarization axis in the plane. The cover glass was bent which induced a tensile or compressive strain of approximately  $1 \times 10^{-3}$  on the sample. The switching experiment was made under parallel polarizers with a compensator. The sample was aligned in such a way that the direction of tensile (or compressive) stress was at  $45^\circ$  to the axis of the polarizer. The ceramic was poled with pulses of up to 45 kV/cm. (All the fingers of the top and the bottom electrodes were joined in common for simplicity of testing.) The polarity of the switching field was then reversed. The magnitude and the width of the switching pulse were varied. A pulse with a field of 45 kV/cm with a pulse width of 4~5  $\mu$ sec would give a better



Figure 18 A PLZT sample with top and bottom crossed interdigital finger array electrodes.

contrast difference between the T-state (ON state) and the L-state (OFF state) in the square overlapped areas. Too long a pulse width would reduce the contrast difference, because the polarization would tend to align in the opposite direction. Areas surrounding the overlapped areas also exhibited contrast effect due to the fringing field. Although a contrast difference was observed, the ratio was too low to be acceptable for a practical display purpose.

The difficulty of the test structure just mentioned above with simply X-Y crossed electrodes was that light would transmit through the dead areas around the overlapped square display elements. This would destroy or distort the information. A simple way to solve this problem was to block these dead areas with a non-transparent material. This was done by depositing a thin layer of GaAs followed by another thin layer of insulating  $\text{SiO}_2$  layer on PLZT ceramics. The detailed fabrication processes were already discussed in Section IV. After etching out the display windows, which were 10 mils by 10 mils, a transparent indium oxide-tin oxide layer was deposited on both surfaces. Figure 19 shows one of the finished samples. For actual X-Y matrix address, the transparent oxide layers on both surfaces had to be etched, delineated into finger-type electrodes crossed with respect to each other. In our test devices, we simply used the whole layer as the electrode. The contact was made with a 2-mil gold wire which was bonded on the transparent electrode with silver paste. The switching experiments on these samples were similar to those used on testing the devices with semi-transparent electrodes.

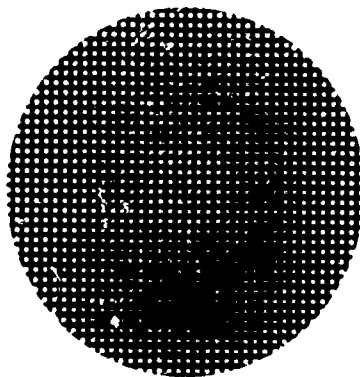


Figure 19 A PLZT sample with 10 mils by 10 mils windows.

It was found that the switching speed of the device was very slow. The maximum optical contrast ratio between on "ON" and "OFF" states under a tensile strain of  $7 \times 10^{-4}$  was only 2.3. The sample was brittle so the maximum applicable tensile strain was limited. Furthermore, a piezoelectric strain was generated when poling fields were applied. The poling field used was about 10 kV/cm and the switching field was about 5 kV/cm. Attempts to increase the dc poling field to 15 kV/cm under a tensile strain of  $7 \times 10^{-4}$  resulted in cracking of the sample caused by this high piezoelectric strain.

#### c) Tests on PLZT Coarse-Grained Ceramics

The second of PLZT ceramic devices tested were made from coarse-grained ceramics. The device utilizes a longitudinal electro-optic scattering effect.<sup>(29)</sup> The maximum transmission or lowest light scattering occurs when the polarization is in the same direction as that of the incident light. The device exhibits the capability of storing photographic images with reasonably high resolution and good gray scale.<sup>(29)</sup> Several advantages of this device are simplicity of fabrication, no requirement of transverse electric field or strain bias, noncritical tolerances on plate thickness, elimination of the polarizer and analyzer and ability to use white light sources for viewing and projection. Because of these advantages the new device approach was undertaken in our display study using coarse-grained (grain size  $> 4 \mu\text{m}$ ) PLZT ceramics.

The coarse-grained ceramics as supplied by Honeywell Company were chemically prepared and hot pressed in an oxygen atmosphere (CP-DX-HP).

After being received, they were lapped and polished on both surfaces and then annealed in air at 700°C for one hour, as described in Section IV. Two studies were made. One involved measurement of the contrast ratio versus the switching electric field, and the other the contrast ratio versus the ceramic thickness.

The experiments on contrast ratio versus the switching electric field were made on samples with semi-transparent gold electrodes on the two major surfaces. The gold electrodes were about 0.5 cm in diameter. The grain size was approximately 4  $\mu\text{m}$ , as shown in Fig. 5. A Vickers tungsten halogen lamp was used as the light source which was placed on one side of the ceramic plate. The aperture at the light source was adjusted such that a light beam of diameter less than 0.5 cm was incident on the sample electrode. An S-20 photodetector with angular aperture of approximately 5° was used to measure the intensity of the light transmitted along an axis normal to the major surfaces.

The ceramic was poled with a field of 10 kV/cm. The sample was then switched with opposite fields increasing from 0 to -10 kV/cm. The intensity of the light transmitted was recorded at each switching field. Figure 20 shows the contrast ratio versus the switching electric field measured on a 100  $\mu\text{m}$  sample. The contrast started decreasing with increasing switching field. At a field of about 3.5 kV/cm the intensity was the lowest. Beyond that field, the intensity increased very rapidly again due to the realignment of the polarization in the opposite direction. The maximum contrast ratio was about 5.2 on this 100  $\mu\text{m}$  sample. The shape of the contrast ratio versus

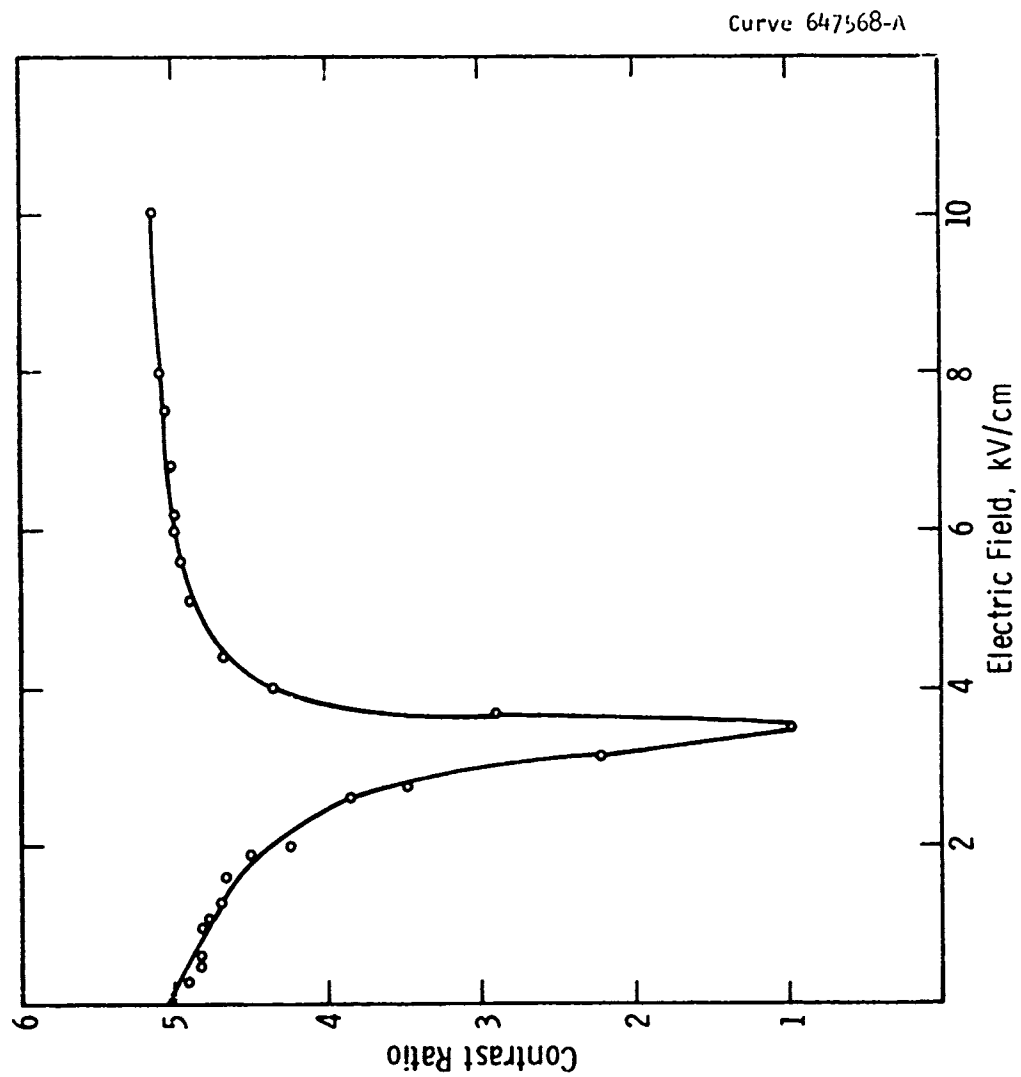


Figure 20 Contrast ratio versus switching electric field measured on a 100  $\mu\text{m}$  coarse-grained sample.

electric field curves for samples of other thicknesses was in general the same. Figure 21 shows the maximum contrast ratio versus the thickness measured on our samples together with that obtained by Smith and Land <sup>(29)</sup> on samples prepared at Sandia. Three thicknesses: 100, 200 and 300  $\mu\text{m}$  were studied. The data were indicated by the square marks. The main reason of lower contrast ratio on our samples was attributed to smaller grain size than that of Smith and Land (see Fig. 6).

#### V.2 Test Results on Epitaxial Bismuth Titanate Films

The test structure used for bismuth-titanate display devices consisted of an interdigitated (IDT) electrode array which we so aligned that the direction of the finger electrodes was at 45 degree with respect to the a and c axes of the film. This structure was fabricated as follows. A Ti-Au multilayer was evaporated on the (110)  $\text{MgAl}_2\text{O}_4$  substrate before the bismuth titanate film was grown. An interdigitated array, which served as the bottom electrode, was delineated with photolithographic techniques, giving 25  $\mu\text{m}$  fingers separated by a 50  $\mu\text{m}$  gap. The active area was about 0.5 cm by 0.6 cm. Each finger was terminated in a 100  $\mu\text{m}$  square contact pad located alternatively at both ends. The epitaxial bismuth titanate layer was then grown on the substrate by the method described in Section IV. Regions of titanate layer over the contact pads were removed by etching in  $\text{HCl}$ . This permitted electrical contact to the bottom electrodes. An upper matching Al array was fabricated with the same mask lying exactly over the bottom one.

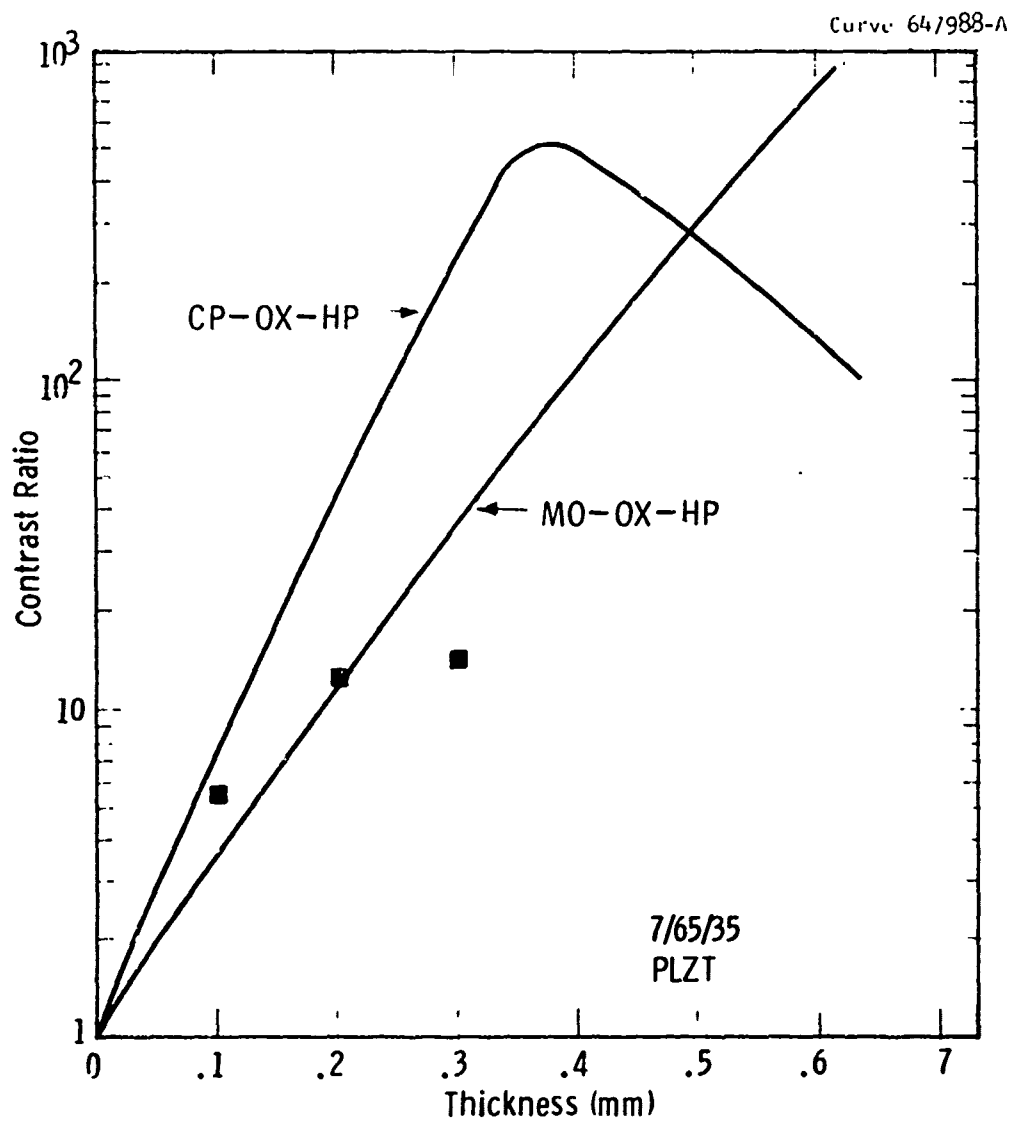


Figure 21 Maximum contrast ratio versus the sample thickness.

The principle of operation of the test structure can be explained from a unit cell enclosed in the dotted lines, as illustrated in Fig. 22. Each unit cell consists of two outer electrodes with one center electrode which divides the active area into two regions. To operate the structure, the outer electrodes are grounded. A field high enough to switch both the a and c polarization components is then applied to all the center electrodes, resulting in a poled structure in the two active regions of each cell. The resulting polarization directions are electrically opposed but the resulting antiparallel orientations of the indicatrix are optically equivalent. Switching of a particular cell is effected by addressing its center electrode with an opposite lower field sufficient to reverse only the low coercive force c-axis polarization components in each region. This reversal produces the same tilt in both of the indicatrices and thus a cooperative change in optical transmission.

For simplicity of the switching experiment, we connected all the center electrodes together. A voltage of +450 volts was then applied to the common center electrode to pole all active regions into a single domain state. The sample was then switched with -225 volts, applying to the common center electrode again. This switched only the c polarization components. If the film was positioned in an extinction position first, the switching would change the film to a transmission state. The light transmissions of the two states were measured with a S-20 photodetector.

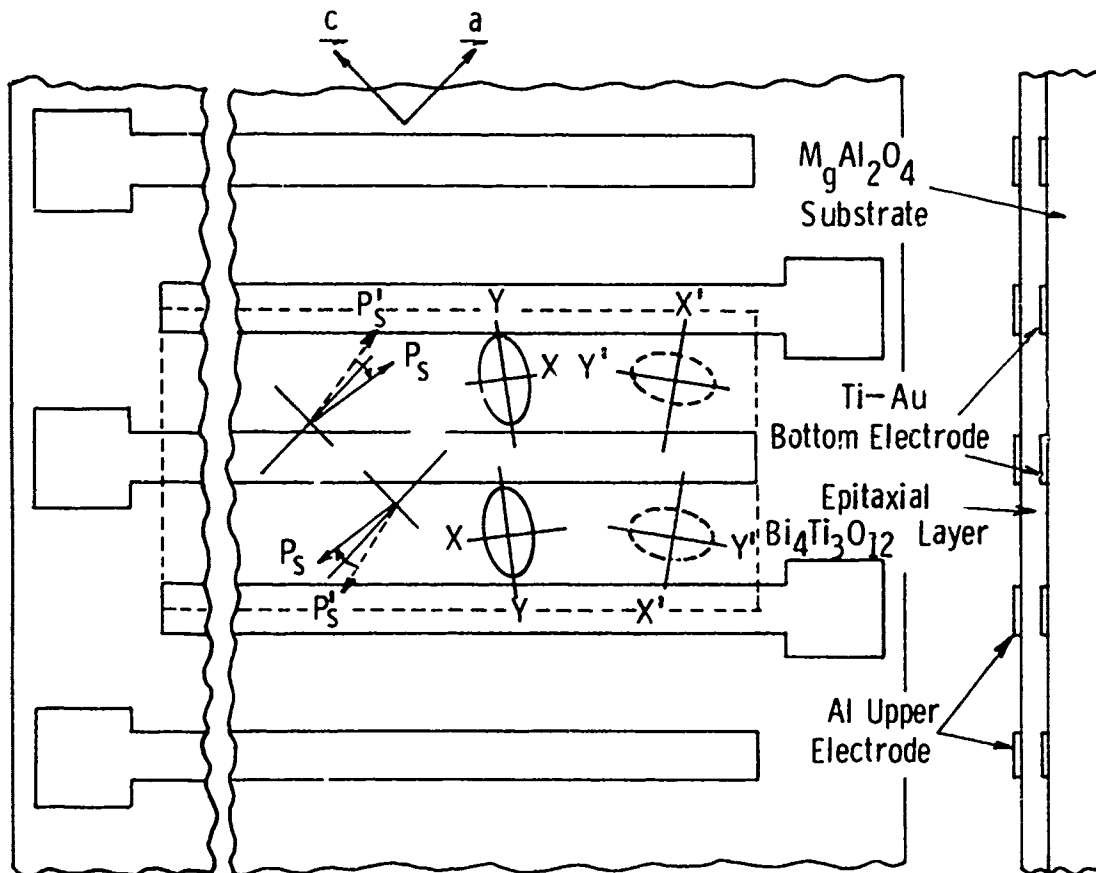


Figure 22 The test structure used to observe the contrast effect of epitaxial (010) bismuth titanate films.

The maximum contrast ratio achieved on bismuth-titanate devices was 7 to 1 with a poling field of 120 kV/cm and a switching field (opposite polarity) of 60 kV/cm. At higher switching fields the contrast ratio gradually decreased due to the progressive reversal of the a-axis component of polarization, which tilted the optical indicatrix back into antiparallelism with the original extinction setting. Figure 23 shows the contrast ratio versus switching electric field obtained from a bismuth titanate device.

### V.3 Experimental Display Structures

The experimental display structures for both the PLZT and bismuth titanate devices were designed to operate with the X-Y matrix addressing scheme. The PLZT coarse-grained ceramics were mechanically lapped and polished. The thickness was about 200  $\mu\text{m}$ . They were annealed at 700°C for one hour in air. After annealing, the GaAs + SiO<sub>2</sub> multilayer was deposited. Display windows of 10 mils by 10 mils were opened. (See Fig. 19). (To get a better resolution on the display picture the size of the windows will be optimized in the later study). A tin doped-indium oxide layer was deposited on each surface and was then etched with photoresist techniques into an array of 10 mil wide bar electrodes spaced at 10 mils. These bar electrodes all made contacts to 10 mil square windows. The bar electrodes on both surfaces were crossed so that the display elements can be addressed with the X-Y matrix addressing scheme. To operate the display structure, all the display windows will be poled to extinction condition. A selective switching on individual windows will be made by applying a field

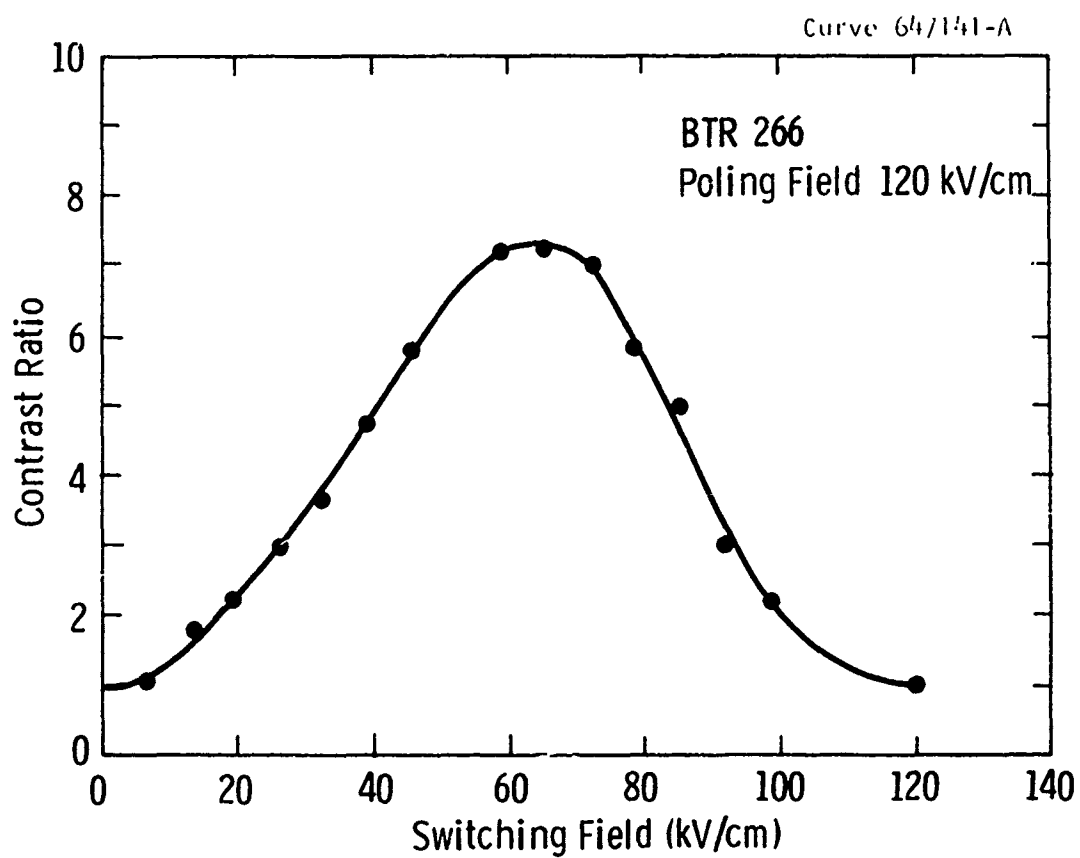


Figure 23 Typical contrast ratio versus switching field on a bismuth titanate film with interdigital electrode structure.

to the proper electrodes to switch them completely or partially. The operation can be controlled with an external X-Y driving circuit or shift registers.

The experimental display structure for bismuth titanate devices operated with X-Y matrix scheme is shown in Fig. 24. The operation mechanism is similar to the test structure using an interdigitated electrode array as described in Section V.2. The fabrication processes are as follows. The bottom Ti-Au electrodes which were 1 mil wide separated by 6 mils were deposited on the  $\text{MgAl}_2\text{O}_4$  substrate at  $45^\circ$  with respect to the (001) axis of the substrate. Bismuth titanate films of about  $10\text{ }\mu\text{m}$  thick were sputtered on with the stress compensation technique. The bismuth titanate layers over the contact pads were etched away to allow access to the bottom electrodes. The upper electrodes which consisted of separated X-addressing electrodes and continuous Y-addressing electrodes were deposited and delineated. They were made of Ti-Au. The continuous electrodes matched exactly with the bottom electrodes. Figure 25 shows a typical sample after the upper electrodes were delineated. To make contact to the X-addressing electrodes, another set of finger electrodes, 1 mil in width and separated by 6 mils, were deposited at 90 degrees with respect to the continuous Y-addressing electrodes. An insulating  $\text{SiO}_2$  layer was used to prevent direct shorting between these electrodes and the continuous upper Y-addressing electrodes. The size of each display element was about 6 mils by 6 mils, shown by the dotted lines. Each element consisted of two active regions.

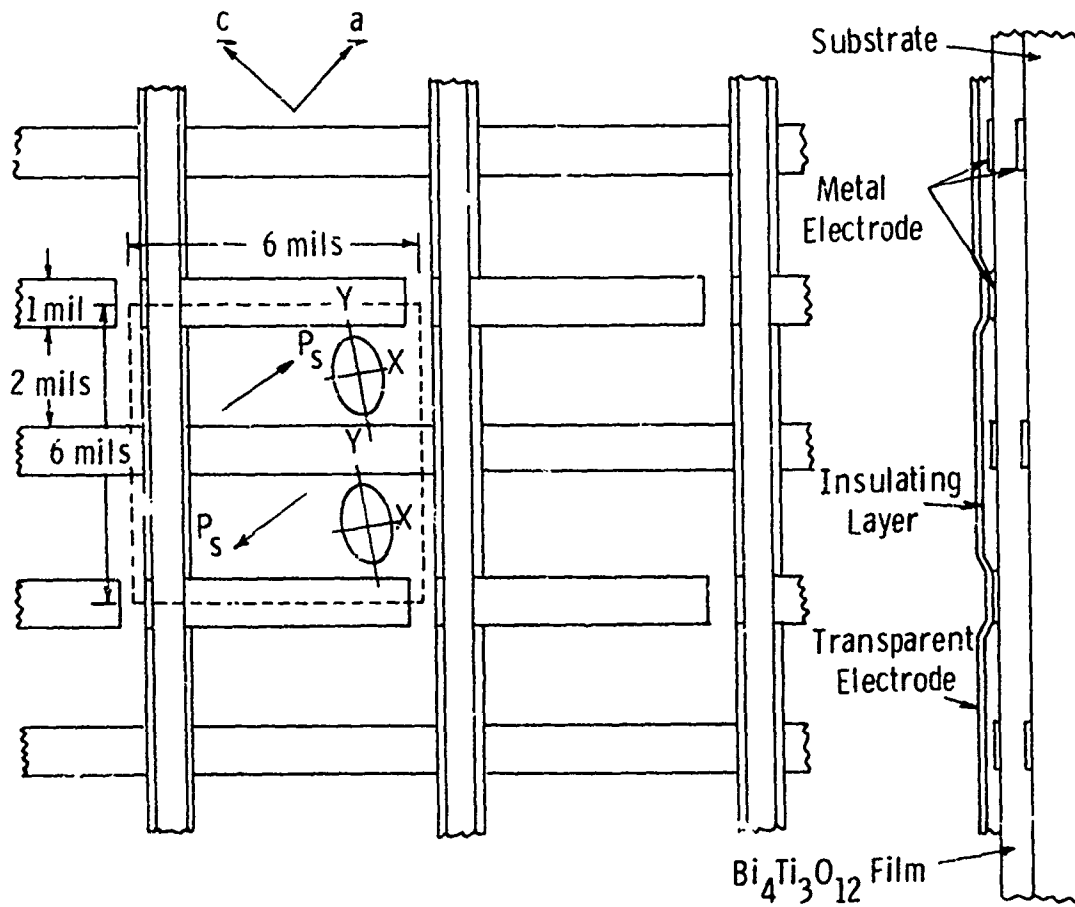


Figure 24 Electrode geometry designed for use with (010) bismuth titanate films with X-Y matrix address.

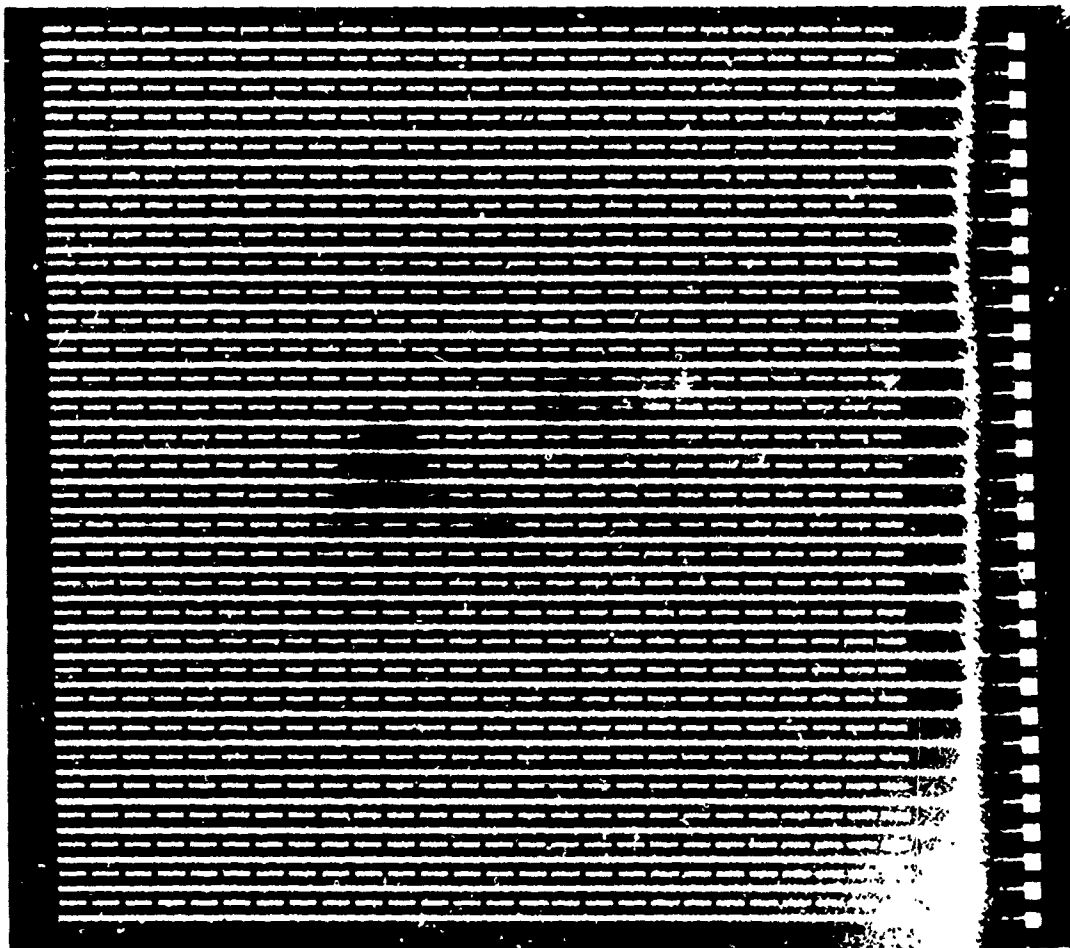


Figure 25    Photograph of a bismuth titanate sample after the top electrodes are delineated.

To operate the device, all display elements are poled first. The device which is placed between crossed polarizers is rotated to an extinction position. An individual cell is then selectively switched with an opposite polarity electric field applied to the corresponding X and Y electrodes. The field is high enough to switch the c polarization components only. The resulting tilt in the optical indicatrix in the two active regions of each cell switches the cell to a transmission state. The grey scale can be obtained by varying the magnitude of the switching field.

## VI. CONCLUSIONS AND RECOMMENDATIONS FOR FURTHER WORK

This study thus far has revealed that the principal difficulties to be overcome in the construction of a high contrast, high brightness display lie in the shortcomings of the ferroelectric material, and in the case of optical address, in the problem of fabricating high dark resistivity, light-sensitive photoconductor layers. Considerable progress has been made both in the evaluation of commercially available PLZT ferroelectric ceramics, and in the Westinghouse program for the growth of epitaxial bismuth titanate layers. In the case of PLZT the emphasis has changed from use of the birefringent mode with fine grained ceramics to the light scattering mode recently discovered for coarse-grained materials. Rapid progress now being achieved with the Honeywell coarse-grained ceramics suggests that these should supply a high contrast display medium in the near future. However, questions still remain to be answered concerning the nature of optical contrast and limitations on the angle of view for this mode of display.

Much has been accomplished in the area of fabrication techniques, both in delineation of electrode masking and electrical insulation. This technology is vital for the successful construction of a working display. During the next phase of this contract the techniques now developed will be applied further to the construction of display devices both in coarse-grained PLZT and in epitaxial bismuth titanate. Although several problems remain to be solved with both of these materials, based upon the present status of our work we feel that a successful demonstration of display capability using the matrix mode of address should certainly be achieved before the end of the program.

#### REFERENCES

1. E. A. Sack, P. N. Wolfe, and J. A. Asars, "Construction and Performance in an ELF Display System" Proc. IRE 47:432 (1962).
2. G. W. Taylor, "The Design and Operating Characteristics of a 1200-Element Ferroelectric-Electroluminescent Display" IEEE Trans. Elec. Dev. ED16:565 (1969).
3. S. E. Cummins, "A New Optically Read Ferroelectric Memory" Proc. IEEE 55:1536 (1967).
4. G. W. Taylor and W. F. Kosonocky, "Ferroelectric Light Valve Arrays for Optical Memories" Ferroelectrics 3:81 (1972).
5. C. F. Pulvari and A. S. De La Paz, "Phenomenological Theory of Polarization Reversal in Ferroelectric  $\text{Bi}_4\text{Ti}_3\text{O}_{12}$  Single Crystal" J. Appl. Phys. 36:1958 (1968).
6. S. E. Cummins, "Switching Behavior of Ferroelectric  $\text{Bi}_4\text{Ti}_3\text{O}_{12}$ " J. Appl. Phys. 37:1754 (1966).
7. S. E. Cummins and B. H. Hill, "Electron Beam Writing of Ferroelectric Domains in  $\text{Bi}_4\text{Ti}_3\text{O}_{12}$  Single Crystals" Proc. IEEE 58:938 (1970).
8. C. E. Land and P. D. Thatcher, "Ferroelectric Ceramic Electro-Optic Materials and Devices" Proc. IEEE 57:751 (1969).
9. G. Marie, "Large Screen Projection of Television Pictures with an Optical Relay Tube Based on the Pockels Effect" Phillip Tech. Rev. 30:292 (1969).
10. D. H. Pritchard, "A Reflex Electro-Optic Light Valve Television Display" RCA Review 30:567 (1969).
11. C. J. Salvo, "Solid State Light Valve" IEEE Trans. Elec. Dev. ED18:748 (1971).
12. S. E. Cummins, "A New Bistable Ferroelectric Light Gate on Display Element" Proc. IEEE 55:1537 (1967).
13. S. E. Cummins and L. E. Cross, "Electrical and Optical Properties of Ferroelectric  $\text{Bi}_4\text{Ti}_3\text{O}_{12}$  Single Crystals" J. Appl. Phys. 39:2268 (1968).
14. W. J. Takei, N. P. Formigoni, and M. H. Francombe, "Preparation and Epitaxy of Sputtered Films of Ferroelectric  $\text{Bi}_4\text{Ti}_3\text{O}_{12}$ " J. Vac. Sci. Tech 7:442 (1970).

15. S. Y. Wu, W. J. Takei, M. H. Francombe and S. E. Cummins, "Domain Structure and Polarization Reversal in Films of Ferroelectric Bismuth Titanate" *Ferroelectrics* 3:217 (1972).
16. W. J. Takei, S. Y. Wu and M. H. Francombe, "Optimization of Epitaxial Quality in Sputtered Films of Ferroelectric Bismuth Titanate" To be published.
17. S. E. Cummins and T. E. Luke, "A New Method of Optically Reading Domains in Bismuth Titanate for Display and Memory Applications" *IEEE Trans. Elec. Dev.* ED18: 761 (1971).
18. G. W. Taylor and A. Miller, "Feasibility of Electro-optic Devices Utilizing Ferroelectric Bismuth Titanate" *Proc. IEEE* 58:1220 (1970).
19. A. W. Smith and G. Burns, "Optical Properties and Switching in  $Gd_2(MoO_4)_3$ " *Phys. Lett.* 28A:501 (1969).
20. S. E. Cummins, "Electrical, Optical, and Mechanical Behavior of Ferroelectric  $Gd_2(MoO_4)_3$ " *Ferroelectrics* 1:11 (1970).
21. H. J. Borchardt and P. E. Burstedt, "Ferroelectric Rare Earth Molybdates" *J. Appl. Phys.* 38:2057 (1967).
22. A. Kumada, "Optical Properties of Gadolinium Molybdate and Their Device Applications" *Ferroelectrics* 3:115 (1972).
23. H. Iwasaki, K. Sugii, T. Yamada, and N. Niizeki, "5 PbO.3GeO<sub>2</sub> Crystal: A New Ferroelectric" *Appl. Phys. Lett.* 18:444 (1971).
24. H. Iwasaki and D. Sugii, "Optical Activity of Ferroelectric 5 PbO.3GeO<sub>2</sub> Single Crystals" *Appl. Phys. Lett.* 19:92 (1971).
25. P. D. Thatcher and C. E. Land, "Ferroelectric Electro-optic Ceramics with Reduced Scattering" *IEEE Trans. Elec. Dev.* ED-16:515 (1969).
26. J. R. Maldonado and A. H. Mertzler, "Ferroelectric Ceramic Light Gates Operated in a Voltage-Controlled Mode" *IEEE Trans. Elec. Dev.* ED-17:148 (1970).
27. A. H. Mertzler, J. R. Maldonado and D. B. Fraser, "Image Storage and Display Devices Using Fine Grain Ferroelectric Ceramics" *Bell Syst. Tech. J.* 49:953 (1970).
28. J. R. Maldonado and A. H. Mertzler, "Strain-biased Ferroelectric Photoconductor Image Storage and Display Devices" *Proc. IEEE* 59:368 (1971).
29. W. D. Smith and C. E. Land, "Scattering Mode Ferroelectric Photoconductor Image Storage and Display Devices" *Appl. Phys. Lett.* 20:169 (1972).

30. G. H. Haertling, "Improved Hot Pressed Electro-optic Ceramics in the (Pb, La) (Zr, Ti) O<sub>3</sub> System" J. Am. Cer. Soc. 54:303 (1971).
31. H. Diamant, K. Drenick and R. Pepinsky, "Bridge for Acoustic Measurement of Ferroelectric Hysteresis" Rev. Sci. Instr. 28:30 (1957).
32. G. H. Haertling and C. E. Land, "Hot Pressed (Pb, La) (Zr, Ti)O<sub>3</sub> Ferroelectric Ceramics for Electro-optic Applications" J. Am. Cer. Soc. 54:1 (1971).
33. E. C. Subbarao, "Ferroelectricity in Bi<sub>4</sub>Ti<sub>3</sub>O<sub>12</sub> and Its Solid Solutions" Phys. Rev. 122:804 (1961).